



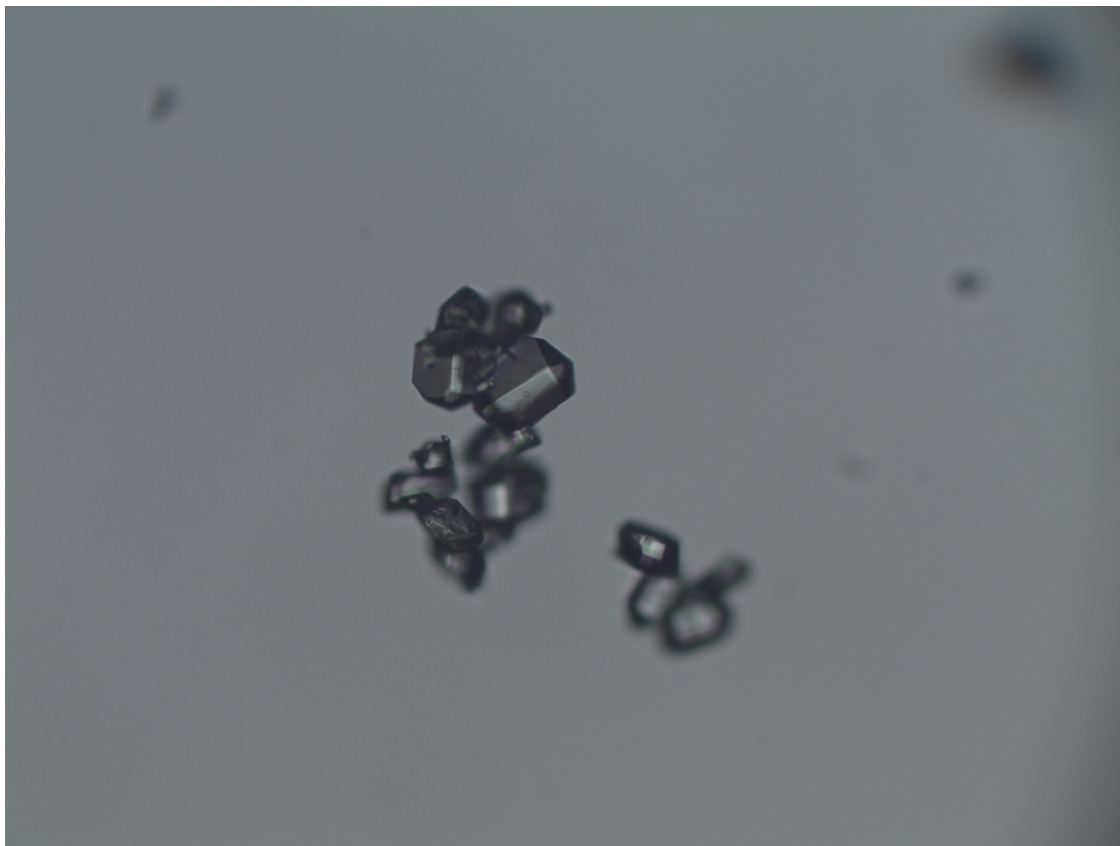
Stockholm
University

Bachelor Thesis

Degree Project in
Earth Science 15 hp

The effect of solution recycling on the precipitation of ikaite and on its role as a reactive intermediary for carbon capture and storage.

Johannes Steenman



Stockholm 2023

Department of Geological Sciences
Stockholm University
SE-106 91 Stockholm

Table of Contents

Abstract	3
1. Introduction.....	3
1.1 Carbonates	3
1.1.1 Anhydrous Calcium Carbonate.....	4
1.1.2 Hydrous Calcium Carbonate	5
1.2 Ikaite its applications and uses.....	7
1.2.1 Ikaite as paleoenvironment indicator.....	7
1.2.2 Ikaite as potential reactive intermediary for carbon capture and storage.....	7
2. Aim.....	9
3. Methods.....	9
3.1 Experiments.....	9
3.1.1 Material collection.....	10
3.1.2 Experimental set up.....	11
3.2 Water analysis and PhreeqC.....	13
3.3 XRD.....	13
4. Results	14
4.1 Experiments.....	14
4.1.1 5°C experimental results	14
4.2 ICP-OES analysis and PhreeqC simulation.....	20
4.3 PhreeqC pH modeling	24
4.3 XRD analysis	25
5. Discussion.....	26
5.1 Potential causes for precipitation	26
5.1.1 The influence of temperature on the precipitation of Ikaite.....	27
5.1.2 The pH regime under which ikaite precipitates.	27
5.1.3 Magnesium and its role as an inhibitor of calcite growth.....	28
5.1.4 Alternative explanations to precipitation patterns.....	31
5.2 Ikaite precipitation in comparison with other CCS methods	34
5.2.1 Percentage of CO ₂ sequestered.....	34
5.2.2 Comparison to other CCS methods.....	35
6. Conclusion.....	36
6.1 Concluding remarks.....	36
6.2 Limitations and further research	37
Bibliography.....	39
Appendices.....	42
Appendix A: Experimental results.....	42
Appendix B: Results from PhreeqC analysis.....	43

Appendix C: Results from PhreeqC analysis.....	44
Appendix D: Calculation support for the sequestration in % of CO ₂	45

Abstract

In this thesis it will be investigated whether recycling of reactant fluid from which ikaite precipitated can increase the yield. And thereby increase CO₂ sequestration, this is done experimentally by recycling the reactant fluid and mixing it with more seawater. The results from the experiment show that recycling the solution from which ikaite precipitates increases yield. With the first recycling seeing a larger amount of precipitate. There are two possible main mechanisms that would cause to pattern to occur. The first is the availability of calcite, which through the introduction of more seawater in the mix became available in greater quantities. Another possible mechanism is that of nucleation. During the experiments it was noted the residual fluid after filtering was not clear. Indicating that particles from the original experiment were introduced during recycling.

1. Introduction

Does ikaite have a role to play in the topical field of carbon capture? In order to provide an answer to this question, in the introduction a literature review will be presented in order to give a general background about research on ikaite. This will be done by first exploring the subject of carbonates, which is subdivided further in anhydrous calcium carbonates and hydrous calcium carbonates to which ikaite belongs. Secondly, ikaite will be discussed in detail with regard to its role as a paleoclimate indicator and as a potential reactive intermediary in carbon capture and storage.

1.1 Carbonates

The carbonate group is the most abundant carbon-bearing mineral in both number of different species and the total crustal volume. Almost all of the carbonates incorporate near-planar (CO₃)²⁻ anions that include an equilateral triangle of oxygen atoms surrounding the carbon atom (Hazen et al., 2013). Approximately 250 different carbonate minerals have been identified, but many of them are exceedingly rare. The more common carbonate minerals incorporate Ca²⁺, Mg, Fe, and Mn (Alderton, 2021). The most abundant types of carbonates are the calcite and dolomite groups which are rhombohedral. However, the orthorhombic carbonates in the aragonite group also play a large role in the carbonate system especially through biomineralization (Alderton, 2021; Hazen et al., 2013). Calcite (CaCO₃) is the most important mineral of the calcite group, others being for example magnesite, rhodochrosite and siderite. The prominence of calcite in the calcite group comes from it being one of the most widely occurring minerals on Earth (Chen and Xiang, 2009;

Hazen et al., 2013). Calcite has several hundred crystal forms and occurs in at least three known polymorphs. Calcite and aragonite are found most commonly in nature and vaterite is metastable at ordinary temperatures and pressures (Alderton, 2021; Chen and Xiang, 2009; “Mindat, Calcite,” n.d.). Apart from this, there are also several hydrous forms of calcium carbonate ($CaCO_3$). Among them, ikaite ($CaCO_3 \cdot 6H_2O$) and its pseudomorphs, and monohydrocalcite ($CaCO_3 \cdot H_2O$) are the most common in the hydrous carbonate group (Hazen et al., 2013). Finally, amorphous calcium carbonate (ACC) is commonly seen as the precursor phase in calcium carbonate mineralization (Gebauer et al., 2008).

1.1.1 Anhydrous Calcium Carbonate

As noted, calcium carbonate is one of the most common minerals on Earth, as one of the three polymorphs: calcite, aragonite and vaterite. It has a multitude of applications, such as in paper as well as playing an important role in the carbon cycle (Chen and Xiang, 2009; Falkowski et al., 2000). It is most common within sedimentary rocks, both as the principal mineral, such as in limestone, but also as a natural cementing agent. Calcite fulfils the role of cementing agent in for instance many siliceous sandstone and shale units that have been deposited under marine conditions. It also occurs in metamorphic rocks such as marble and occurs in carbonate-rich igneous rocks called carbonatites (Hazen et al., 2013; Jones et al., 2013). The wide range of different types of rocks and settings calcite occurs in, explains the high variety of morphologies of this mineral. The morphology of calcite is highly affected by the kinetics of crystal growth (Gopi et al., 2013; Gutjahr et al., 1996; Zhang and Dawe, 2000), but much remains unknown due to the high variety of factors influencing the precipitation of calcite.

Aragonite and vaterite are the less stable polymorphs of calcium carbonate. Vaterite is the least stable and aragonite can be placed between calcite and vaterite. Aragonite is commonly found in marine sediments where it is metastable with respect to calcite. It is thought that recrystallization to calcite is inhibited by the presence of Mg, which is present in seawater in significant concentrations (Gutjahr et al., 1996). Vaterite is a much rarer mineral but, as with calcite and aragonite, it also occurs through biomineralization. However, it is instable under ambient conditions. As highlighted by Hazen et al., (2013), it is the preferred mineral used for storage of material critical to skeletal growth. This is due to it being stable under the influence of a variety of hydrophilic organic molecules.

1.1.2 Hydrous Calcium Carbonate

The hydrous calcium carbonate minerals are of considerable interest for the present research into carbon capture and storage methods, due to their role as precursors to stable carbonate minerals. Monohydrocalcite is a metastable mineral under all conditions, and forms predominantly in freshwater environments (Sekkal and Zaoui, 2013). Ikaite has been first described and named by Pauly, (1963) who found the mineral in the Ikka fjord in southwest Greenland as tufa columns. Furthermore, it is found in two other environments; in sea ice and in lakes such as Mono Lake, California, as well as in sediments (Bischoff et al., 1993b; Dieckmann et al., 2008; Vickers et al., 2018). Ikaite is a metastable calcium carbonate mineral ($\text{CaCO}_3 \cdot 6\text{H}_2\text{O}$). The consensus is that the mineral only forms in nature under specific conditions. This is based on the observation that ikaite has only been found in the range of -2 to 7°C in nature and at high alkalinity.

Experimentally, it has been shown that ikaite is stable under high pressures and low temperatures (Bischoff et al., 1993a; Kawano et al., 2009; Marland, 1975; Shahar et al., 2005). As ikaite is only stable under high pressure, it is remarkable that it occurs at surface pressure in the Ikka fjord.

The crystal structure has been defined by Dickens and Brown, (1970) using synthetic ikaite and later refined by Hesse et al., (1983) using natural ikaite. Hesse found and affirmed that ikaite, $[\text{CaCO}_3 \cdot 6\text{H}_2\text{O}]$, is monoclinic, $C2/c$ with $a = 8,792(2)$, $b = 8,310(2)$, $c = 11021(2)\text{\AA}$, $\beta = 110,53(5)^\circ$, $Z = 4$. These quantities are still being used today to describe the structure of ikaite. The formation of the pseudomorphs is dependent on the conditions to which ikaite is exposed. When it is exposed to higher temperatures it tends to form aragonite. When exposed to air at higher temperature it is transformed into pure calcite or into calcite-vaterite admixtures (Purgstaller et al., 2017).

During expeditions to Ikka Fjord, it was found that ikaite precipitated from a mixture of seawater and spring water that came from the Grøndal-Ika igneous complex that flanks the fjord. The conditions in the Ikka fjord under which the tufa columns form are relatively stable year round (Buchardt et al., 2001; Hansen et al., 2011; Trampe et al., 2016).

As mentioned, ikaite has also been found in sea ice. It was first discovered in 2008 in Antarctica (Dieckmann et al., 2008) and shortly thereafter in 2010 in Arctica. Ikaite forms in hyper saline brine pockets within the sea ice, as both idiomorphic and xenomorphic crystals. The xenomorphic crystals are most likely constrained by the brine pocket dimension (Dieckmann et al., 2010). The role of ikaite in sea ice is not fully understood. First, the proposition was that ikaite formed in sea ice due to phosphate inhibition, although later it was shown that this was not case. The abundance of ikaite in sea ice may have a key role in the global carbon cycle. This was demonstrated by the

observation that after melting of the sea ice a positive influence on the CO₂ uptake was found, due to ikaite precipitation which lowered the pCO₂ levels of the surface water.

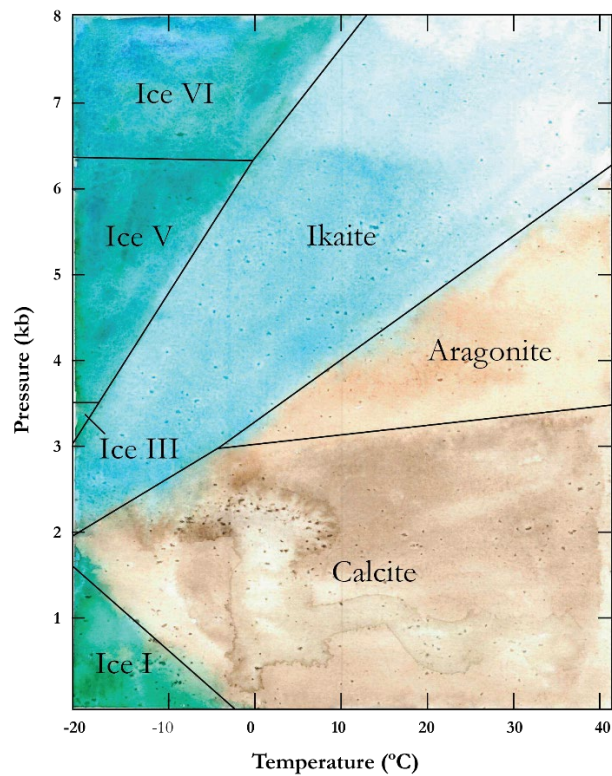


Figure 1 Figure showing the phase diagram for ikaite, aragonite and calcite. With pressure in kb on the Y axis and temperature in Celsius on the X axis. From Bischoff et al., (1993a) and Marland, (1975)

Other important parameters which influence the precipitation of ikaite are pH and Mg concentrations. The influence of phosphate and SO₄ as calcite growth inhibitors in the formation of ikaite have been suggested in the past. However, these are probably not the inhibiting factors for precipitation. This was demonstrated in experiments where phosphate was removed and ikaite continued to precipitate instead of calcite. Furthermore, it was shown in experiments by Tollefsen et al., (2018) that SO₄ was not a factor in the precipitation of ikaite. Instead, the Mg concentration and pH are the main controls of ikaite precipitation with both a higher pH and Mg concentration contributing to ikaite precipitation. Furthermore, experiments conveyed that in a natural seawater and synthetic spring water mixture with a Mg concentration of 22.8 ± 0,50 mmol/kg required a pH of 9.3 or above for ikaite to precipitate. The presence of Mg is suggested to be the primary kinetic factor which allows ikaite formation, as it appears to inhibit the nucleation and/or growth of calcite. The interconnection between Mg²⁺ concentration and pH at 5°C had a kinetic boundary for the appearance of ikaite in the precipitate, which is shown by the following power law: $C_{Mg} = (2,68 \times 10^{15}) pH^{-14,49}$, where C is the concentration of Mg in mmol/kg (Tollefsen et al., 2018). This

indicates that Mg and pH are important factors to consider when performing experiments with ikaite.

1.2 Ikaite its applications and uses

Due to the unique conditions ikaite forms under, it can be used in various applications. Two of such applications can be in paleoclimate research and in carbon dioxide removal (CDR) technology.

1.2.1 Ikaite as paleoenvironment indicator

The use of ikaite or more specifically glendonite as a paleoclimate indicator has been studied for a long time. It was first thought to be a good indicator of temperature as demonstrated by Swainson and Hammond, (2001) with ikaite in nature forming at temperatures between -2 and 7°C. Yet, a mere vicennial later this idea has been contested by research showing that ikaite can form at temperatures up to 35°C (Tollefsen et al., 2020). Moreover, in earlier experiments it was shown that at a set pH of 8,3 and defined aqueous molar Mg/Ca ratios, ikaite formed in temperatures up to 12°C. (Purgstaller et al., 2017). These discoveries question the use of glendonite, which is a pseudomorph of ikaite, as a paleotemperature indicator.

Glendonites have been used as paleoclimate indicators with support from other sources such as stratigraphy and isotopic evidence to use the pseudomorph of ikaite as an indicator of lower temperatures during the Cretaceous and Eocene greenhouse (Vickers et al., 2018, 2020, 2019). As such, due to its contested status as a paleoclimate indicator, research has been performed on the breakdown of ikaite to glendonite to review if it can be used as a reliable paleoclimate indicator. This has shown that ikaite in air may undergo quasi – solid state transformation when temperatures are gradually raised. And as such clumped isotope thermometry can be used on ikaite-derived calcite to reconstruct ikaite growth temperatures (Vickers et al., 2022).

1.2.2 Ikaite as potential reactive intermediary for carbon capture and storage

Another application of ikaite could be as a reactive intermediary for carbon capture and storage. Carbon capture and storage works on the premises of capturing carbon and storing it, for thousands of years or longer, in geological formations. One such technique relies on the pumping of CO₂ into subsurface sedimentary basins. An example of this is the project at Sleipnir Norway, where CO₂ has been injected into the Utsira sandstone below the sea floor since 1996 (Gislason

and Oelkers, 2014; *IPCC special report on carbon dioxide capture and storage*, 2005). An issue with this technique is that the transformation to carbonate minerals in these kinds of systems is very slow which creates the risk of leakage (Gislason and Oelkers, 2014; Lane et al., 2021; Matter et al., 2016).

A proposed solution to the issue of leakage is mineral carbonation. This involves converting CO₂ to a solid inorganic carbonate using chemical reactions. This can be done through the use of magnesium oxide (MgO) and calcium oxide (CaO) which are present in naturally occurring silicate rocks such as serpentinite and olivine (*IPCC special report on carbon dioxide capture and storage*, 2005). In this setup, which is called ex situ mineral carbonation, the Ca and Mg bearing minerals are extracted and processed before being reacted with CO₂ (Chang et al., 2017).

One method employing this approach, but not needing mining, is applied in Iceland. In the project, which is called CarbFix, CO₂ is pumped into basaltic layers. The process relies on in situ mineral carbonation. In the initial phase the CO₂ was obtained from a nearby thermal plant and transported to the injection location (Kintisch, 2016). Later the option for direct air capture (DAC) was added to the pilot with the company Climeworks. In this method CO₂ is directly filtered from the air and injected in the basalt (Gutknecht et al., 2018). The results from the experiments have shown that the mineralization occurred much faster than initially thought, with near complete in situ CO₂ mineralization in two years (Gislason and Oelkers, 2014; Matter et al., 2016). This development, however, comes with its own limitations such as scale and economic feasibility issues. Also, another issue is the transport of CO₂ from source locations to suitable areas for injection.

A method with the potential to avoid some of these issues is described in the patent by Tollefsen and Skelton, (2020). In contrast to the earlier described methods of carbonation, this process does not rely on mineral bedrock and thus has the potential to be employed in locations where the required bedrock does not occur. In this method an aqueous solution with inorganic carbon content of at least 10 mmol/kg, at least 5 mmol/kg Mg²⁺, at least 2 mmol/kg Ca²⁺, and at least 50 mmol/kg Na⁺ is used with the pH of the aqueous solution adjusted to 9.1-10.4. This setup results in 0.17 g/l precipitation at 5-15°C and 0.26 g/L at 20-35°C. One of the main benefits of this method is that, as a reactive intermediary, ikaite reduces the duration of the reactive process from years to hours for carbon storage. From earlier experiments, it was found that a 2:1 solution of 0.1 M Na₂CO₃ and 0.1 M NaHCO₃ and natural seawater are appropriate proxies for the afore described conditions (Stockmann et al., 2018; Tollefsen et al., 2020, 2018). Nevertheless, in unpublished results by Tollefsen, (n.d.), it was shown that only 2% of the CO₂ from the aqueous solution was sequestered, making it a non-viable option for CCS under the testing conditions. One

of the identified limitations was the amount of Ca^{2+} in the solution. A proposed solution to this limitation, which will be investigated in this thesis, is to recycle the aqueous solution and mix it with more seawater.

2. Aim

In this study, my aim is to add to the growing body of literature on potential solutions for carbon capture and storage. More specifically, the aim is to answer the question: Does recycling the solution from which ikaite precipitates increase the yield? This was tested experimentally by recycling the residual fluid and mixing it with more seawater. This is of interest because earlier unpublished work done by (Tollefsen, n.d.) showed that only $\sim 2\%$ of the CO_2 was sequestered despite there being available Ca in solution.

3. Methods

In the section that follows, the methods employed to research the question posed on whether the ikaite yields can be increased will be presented. The first part of this section focusses on the experiments that were performed. Therein, the methodology of the experiments will be explained as well as the rationale behind the steps. In the second part, the focus will be on the analysis of the fluids that were used and produced in the experiments. The analysis was performed by inductively coupled plasma atomic emission spectroscopy and subsequently using the PHREEQC geochemical modelling software. Lastly, the precipitates of the experiments is discussed. These were analyzed using X-ray powder diffraction to differentiate which minerals have precipitated during the experimental stage.

3.1 Experiments

The experiments are based on the methods as described in Stockmann et al., (2018) and Tollefsen et al., (2020, 2018). The authors set up experiments using synthetic spring water and either natural or synthetic seawater in order to mimic conditions as found in the Ika fjord to determine the inhibitors of calcite to allow for ikaite precipitation. The experiments can be divided into three separate phases. The first phase deals with collecting the materials and setting out the experiments. The second phase deals with the running of the experiments at set temperatures, while the third is related to initial data collection.

3.1.1 Material collection

One of the main components of the experiment is natural seawater. As there are no sources of natural seawater on the eastern side of Sweden, the best and most easily reached source was Gothenburg. Therefore, the journey was undertaken to collect approximately 10 liters of seawater. As Göta Älv has its mouth in Gothenburg a location that was adequately away from this had to be chosen in order to avoid collecting brackish water. Hence, the seawater was collected in the archipelago of Gothenburg on the island of Styrösö (figure 2). The seawater was retrieved as far from the shore and as deep as possible in order to avoid the surface layer. This in practice this means approximately 4 meters from the shore and at a depth of 0.5 meters. After retrieval, the seawater was filtered using a Munktell 00M filter and kept refrigerated until it was used. An concern with the locality and the depth of the collected seawater is that there is a high chance that the seawater was surface water. This is a potential cause of error, as the surface seawater can have different concentrations of salts and other dissolved minerals.

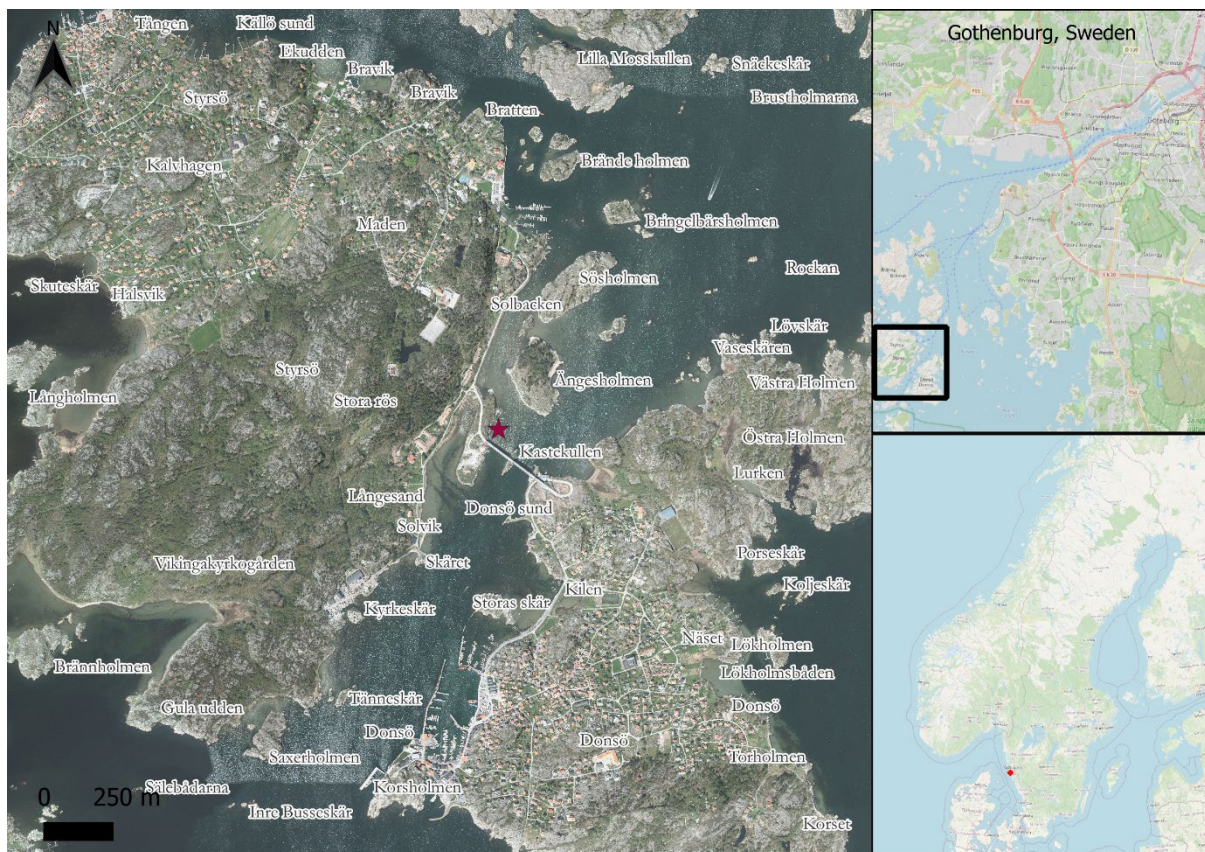


Figure 2 Map over the collection locality on Styrösö Island in the Gothenburg archipelago. The left map shows the islands of Styrösö and Donsö. With the locality where the seawater was collected marked by a red star. The top right inset map shows demarcated area of the left map in relation to Gothenburg. The bottom right map indicates the collection locality in Sweden as indicated by the red dot.

The solution designed to represent a solution containing captured CO₂ for CCS used in the experiments was synthetic and will hereafter be called “spring water”. The synthetic spring water was made up of 0.1 M Na_2CO_3 and 0.1 M $NaHCO_3$ in a ratio of 2:1 within the range of spring waters occurring at Ika fjord as described by Buchardt et al., (2001). The solutions were made by mixing MERCK powders in 1 liter of ultrapure deionized water and kept refrigerated until used.

3.1.2 Experimental set up

The experiment was set up at the Department for Geological Sciences at Stockholm University. Four series of experiments were run with two at 5°C and two at 20°C. The initial experiments were performed by mixing seawater with the synthetic spring water. After these experiments, subsequent experiments were performed using the residual water from the previous experiment mixed with seawater.

The first stage in the experiment is the setup of the temperature baths. The larger model of temperature bath (Julabo F-32) was used to keep the two solutions at a consistent temperature, while the smaller model (Julabo F-25) was used for the reaction vessel. The liquids were mixed using an Isamatic BVK peristaltic pump which was set to run for 80 minutes, pumping approximately 700ml of reactant in each experiment. After each experiment the pH and temperature of the seawater, synthetic spring water or recycled solution and, the reactant water were measured. A HANNA hi 9126 pH meter and an HI-1230B electrode were used for the pH measurement and an HI-7662 sensor was used to measure the temperature. The reactant was set in a 5°C cooling room after the experiment. After leaving the mixture overnight, it was filtered with a Munktell 00 K filter in the cooling room. The filter was left in place for an hour after all of the reactant fluid had been run through to ensure the filter was relatively dry. After this, the filter was placed on a glass dish and left overnight to dry. After drying overnight, the precipitate was weighed and stored in a freezer to ensure the minerals remained stable. For preliminary assessment of the samples, residue from the filter paper was inspected under the microscope. See figure 3 for a visual presentation of the experimental setup. After each experiment the glasswork and containers used were cleaned with hydrochloric acid to prevent contamination into subsequent experiments.

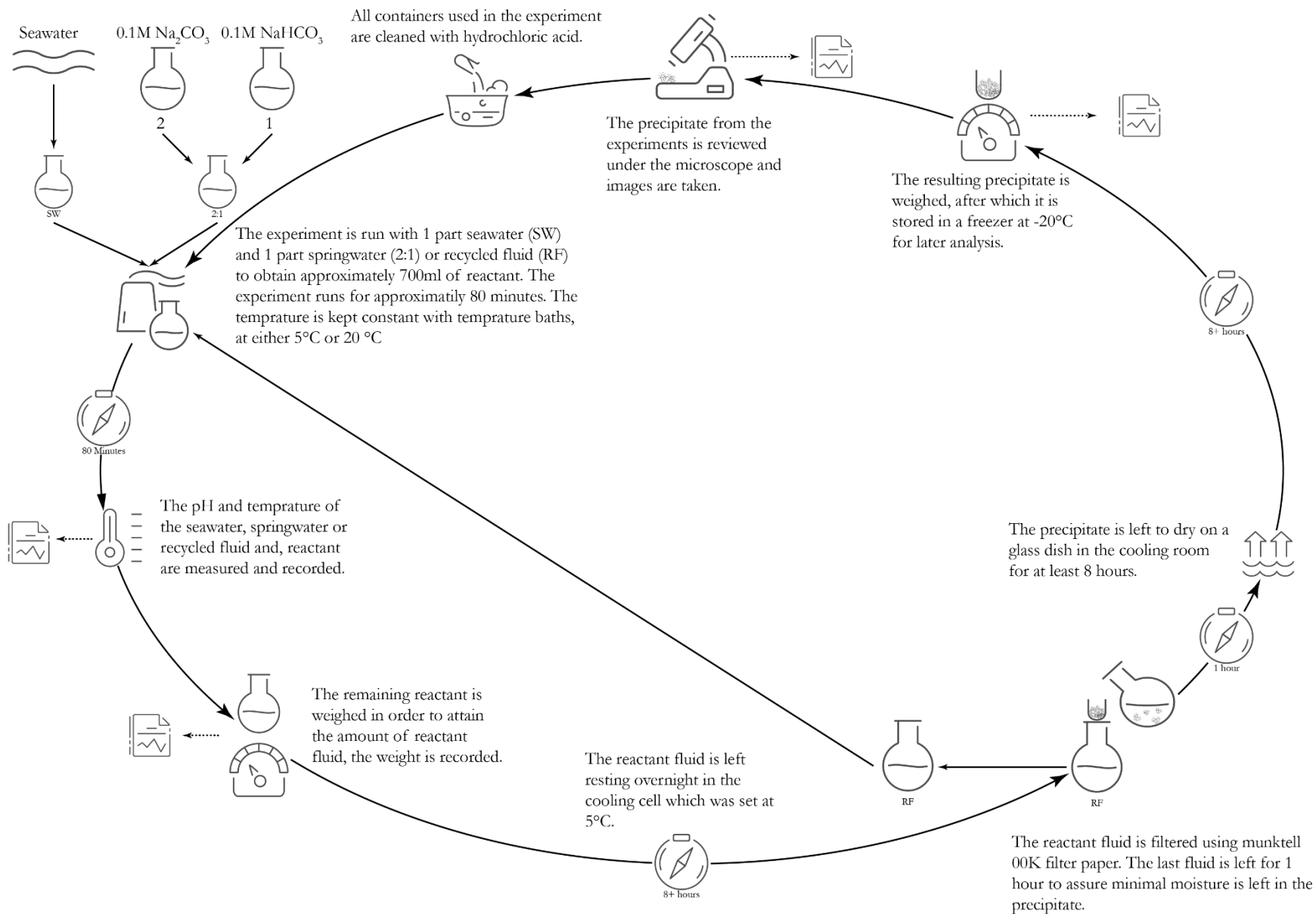


Figure 3 conceptual representation of the methods, illustrated as a cycle to emphasize the recycling of the fluid with more seawater, as indicated by the RF marked figures.

3.2 Water analysis and PhreeqC

The seawater, synthetic spring water and the filtered recycled fluid were analysed using inductively coupled plasma atomic emission spectroscopy (ICP-OES) at Stockholm university. These analyses allow for the detection and quantification of Ca, Na, K, Mg and S concentrations. This was subsequently processed in PhreeqC interactive version 3.7.3 to calculate values for pH and ionic speciation. Saturation indices (SI) were taken from the PhreeqC llnl database, except for ikaite [$\text{CaCO}_3 \cdot 6\text{H}_2\text{O}$], vaterite (CaCO_3) and ACC (CaCO_3). These were added in the “PHASES” of the model. The solubility constants have been taken from Bischoff et al. (1993a) for ikaite, Plummer and Busenberg, (1982) for vaterite and Brečević and Nielsen (1989) for ACC. The SI was set at $\text{SI} = \log(\text{IAP}/\text{Ksp})$, with IAP being the ion activity product and Ksp being the solubility constant. The analyses were performed in a batch after all experiments were completed. In practice this means that there were some weeks between the completion of the experiments and the analysis. This delay may mean that reactions within the recycled fluid have continued to occur. As such this is a potential source for error when considering the available Ca introduced into the recycling experiments. Where more Ca is introduced in the recycling experiments than is indicated by the results from the ICP-OES.

The PhreeqC geochemical model has been employed in order to calculate the pH values of the experiments, as well as the saturation indices of the resulting mixtures. The calculated pH values were used instead of measured pH. As was noted by Tollefsen et al. (2018), the rapid precipitation of the super supersaturated mixture would not allow for accurate pH measurement. To use the results from the ICP-OES in the PhreeqC geochemical model, the values for Cl and C have to be calculated. From the water analysis the values for Na and S are known. Which, with the assumption that the compounds that contain sodium in the water are NaCl, Na₂SO₄ and NaHCO₃ can be used to derive both Cl and C contents. As the values for Na and S are known and each resulting mixture contains 50% seawater and 50% NaCl from the prior solution, the assumption is made that the remaining sodium is associated with NaHCO₃ which allows for the calculation of C and the final calculation for Cl.

3.3 XRD

In order to identify the minerals, powder X-ray diffraction (XRD) patterns were measured with a PANalytical X'pert pro instrument at the Swedish Museum of Natural History in Stockholm. The analysis run took 11 minutes from 0 to 70°. This short timeframe was necessary to prevent the

ikaite from transforming to calcite before the experiment was completed. In addition to this, the sample holder was refrigerated for 10 mins in a freezer (-18°C) to preserve the sample. Mineral identification and quantification (Rietveld refinement) was done using the program HighScore. Rietveld refinement is used for the characterization of crystalline material. The method relies on a characteristic pattern by reflections, which show in intensity and the peak position. Each mineral has a specific pattern of peaks and peak intensity which can be used to identify minerals (Rietveld, 1969). The program uses phase identification based on reference patterns. Identification can be done based on peak positions and/or on the full net profile (Degen et al., 2014). The analysis was performed on site at the Museum of Natural History.

4. Results

4.1 Experiments

The experiments were set up in four series, two at 5°C and two at 20°C. Series 1 and 3 have been performed at 5°C and 2 and 4 at 20°C. As stated earlier, the main objective of the experiments is to determine whether the recycling of the solution from which ikaite precipitates can increase the amount of CO₂ sequestered. The experiments are divided into two distinct segments, the first is the initial experiment. This experiment is marked by an “a” in the graphs and figures. And the recycling experiments, these are all subsequent experiments and are marked by sequential letters after a.

4.1.1 5°C experimental results

Series 1 and 3 were run at 5°C until there was no significant amount (>0.001g) of precipitate after the experiment (Table 1). In both series this was at the 4th experiment, or third recycling, which are marked by a “d”. At this point no more precipitate appeared out of the solution. When running experiment initial experiments (a) there was visible precipitation in the reaction vessel right after the experiment, which was shown by the milky appearance of the solution. After filtering of solution from the initial experiments (a), the liquid was visibly slightly opaque. This liquid was subsequently used in the first recycling (b). In experiment first recycling, precipitation was also visibly occurring during the running of the experiment. However, most of it occurred during the resting period in the cooling room overnight. In this experiment the yield of precipitate was significantly higher than in the initial experiment and any subsequent recycling experiments for both series 1 and series 3. In the second recycling (c) the solution was clear directly after the

experiment and precipitation occurred during the time in the cooling room. As the experiments progressed the pH of the solution steadily declined from around 10.2 to 9.3.

*Table 1 The table below shows the results from the experiments, the table has been broken up into 4 series. The sample name indicates which experiments has been run, mixed water type indicates which fluid seawater was mixed with while temperature indicates the temperature at which the reactions baths were set. Series 1 and 3 were performed at $5\pm 0.5^{\circ}\text{C}$ and series 2 and 4 at $20\pm 2^{\circ}\text{C}$. The solution pH was taken directly after the experiment while the residue is the pH after filtering. *pH was measured and is temperature dependent, approximately accurate to ± 0.1 . ' measured weight in kg ± 0.01 . " precipitate in g ± 0.001 . ** Calculated g/kg from to former two columns.*

sample name	Mixed water type	Temperature $^{\circ}\text{C}$	Solution pH*	Residue pH*	Measured volume kg'	Precipitate" g"	Precipitation g/kg**
Serie 1							
Exp 3-22-a	2:1 Batch 1	5	10.20	10.09	0.654	0.063	0.097
Exp 3-22-b	3-22-a residue	5	9.89	9.85	0.639	0.335	0.523
Exp 3-22-c	3-22-b residue	5	9.68	9.49	0.626	0.057	0.091
Exp 3-22-d	3-22-c residue	5	9.31	9.20	0.580	-	0.000
						Total g/kg	0.711
Serie 2							
Exp 4-22-a	2:1 Batch 2	20	10.09	10.05	0.697	0.056	0.080
Exp 4-22-b	4-22-a residue	20	9.83	9.77	0.682	0.314	0.461
Exp 4-22-c	4-22-b residue	20	9.59	9.38	0.680	0.074	0.109
Exp 4-22-d	4-22-c residue	20	9.21	8.75	0.665	0.042	0.063
Exp 4-22-e	4-22-d residue	20	8.68	8.66	0.648	-	0.000
						Total g/kg	0.712
Serie 3							
Exp 6-22-a	2:1 Batch 4	5	10.15	10.11	0.597	0.047	0.079
Exp 6-22-b	6-22-a residue	5	9.92	9.85	0.589	0.224	0.381
Exp 6-22-c	6-22-b residue	5	9.65	9.52	0.593	0.155	0.262
Exp 6-22-d	6-22-c residue	5	9.28	9.18	0.608	0.000	0.001
						Total g/kg	0.723
Serie 4							
Exp 5-22-a	2:1 Batch 3	20	10.05	9.99	0.656	0.059	0.090
Exp 5-22-b	5-22-a residue	20	9.79	9.74	0.653	0.279	0.428
Exp 5-22-c	5-22-b residue	20	9.57	9.29	0.649	0.066	0.102
Exp 5-22-d	5-22-c residue	20	9.15	8.77	0.684	0.042	0.061
Exp 5-22-e	6-22-d residue	20	8.69	8.74	0.680	-	0.000
						Total g/kg	0.681

In figure 4, the results from series 3 can be seen, in respectively 20 and 40 magnification. During the initial experiment (a) some euhedral crystals were observed with many crystals being subhedral. The proportion of euhedral crystals was higher in the first recycling (b) with crystals being smaller in size. In the second recycling (c), large crystals in a different morphology than the prior two experimental runs were observed. The crystals were larger in size and significantly different in shade. The crystals being a shade of brown and less opaque than in the other experiments. Their shapes were best described as subhedral with some euhedral crystals also occurring. In the third recycling (d), only a small amount of precipitate was observed. This amount was so little that it could not be weighed to any degree of certainty ($>0,001$) and its presence was only confirmed

through the microscope. This contained very few euhedral crystals. On preliminary judgement, all samples seemed to contain ikaite, however, this is discussed further under 4.3 XRD results.

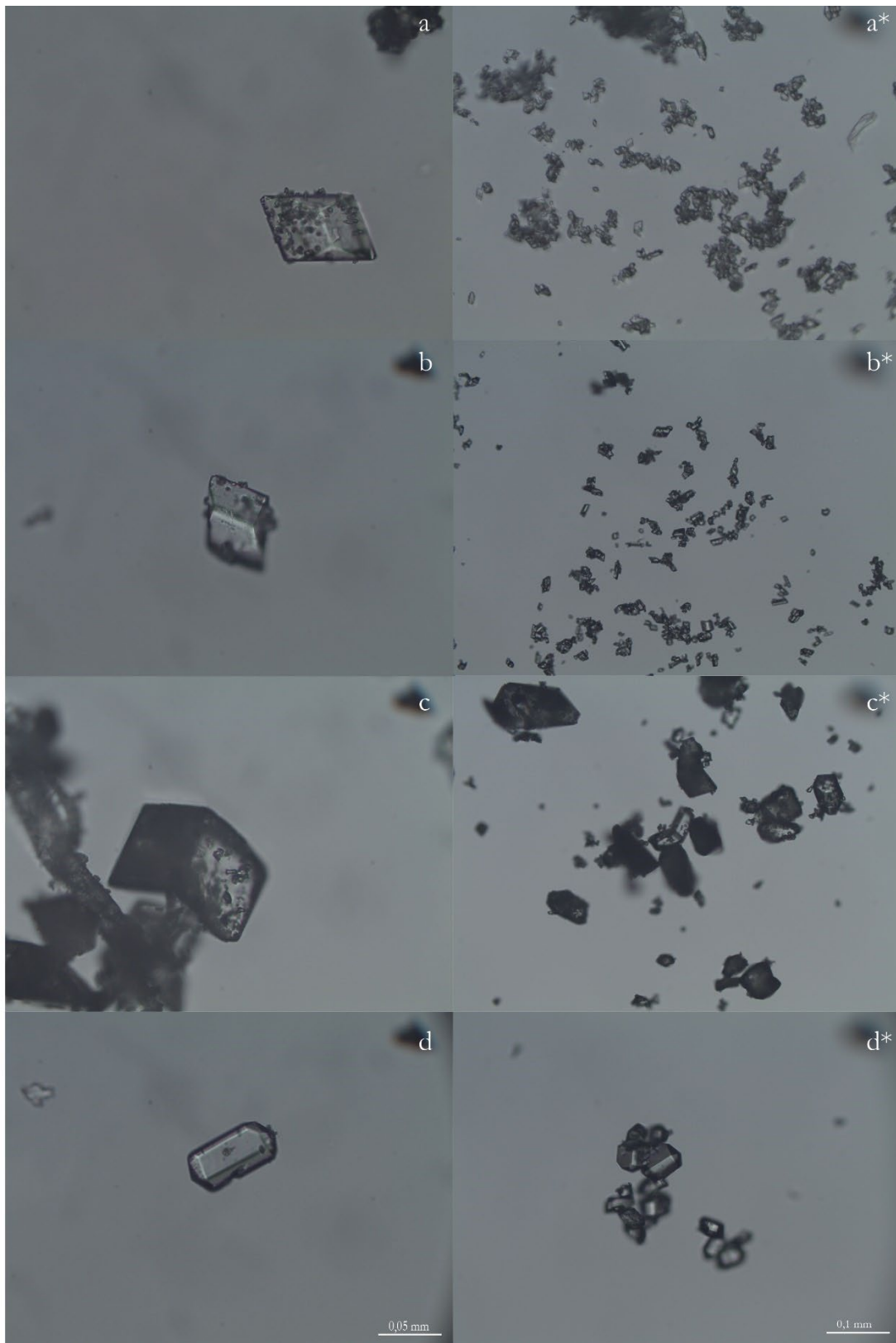


Figure 4 Images from the microscopy photographs, taken at Stockholm University Department of Geology. Using a Nikon microscope and Leica camera. The images on the left side and without a "*" are taken with a 40x magnification objective lens while images on the right side and marked with a "*" are taken with a 20x magnification objective lens. Scale markings at the bottom correspond to all images above. Images are taken from minerals from series 3 as in table 1.

4.1.2 20°C experimental results

Conversely series 2 and 4 were run at 20°C until there was no significant amount ($>0.001\text{g}$) of precipitate after the experiment, see table 1. This was after the 4th recycling experiment (e), in this instance there was no further precipitate present. The experiments showed the same initial pattern as in the series which was run at 5°C. The largest amount of precipitate was produced in the second experiment. However, in these series there was an additional experiment that produced precipitate compared to the ones run at 5°C. The total precipitate for both series was $\approx 0,700\text{ g/kg}$, similar to that at 5°C. The pattern observed of precipitation was that during the initial experiment (a) and the first recycling (b) it was directly visible that there was precipitate which increased after being left overnight. In the second (c) and third (d) recycling this was not the case and precipitation occurred during the resting phase in the cooling room. The pH of the solution dropped steadily from 10,1 to 8,7 over the course of the experiments.

During the preliminary microscopy, subhedral crystals were observed during the initial experiment (a). Exceptionally large euhedral crystals were observed during the first recycling (b), which were on some occasions so large that they did not fit in the 40 magnification. This can be seen on the left image marked “b” (figure 5). In this phase it was also notable that smaller crystals seemed to be attached to the larger crystals. These smaller materials appeared spherical in morphology. The images corresponding to experiment second (c) and third recycling (d) did not show any specific morphology apart from being relatively spherical. However, this material was difficult to discern as it clumped together. This material also had a darker color than observed in the earlier experiments, the images marked “c” and “d” correspond to these experiments.

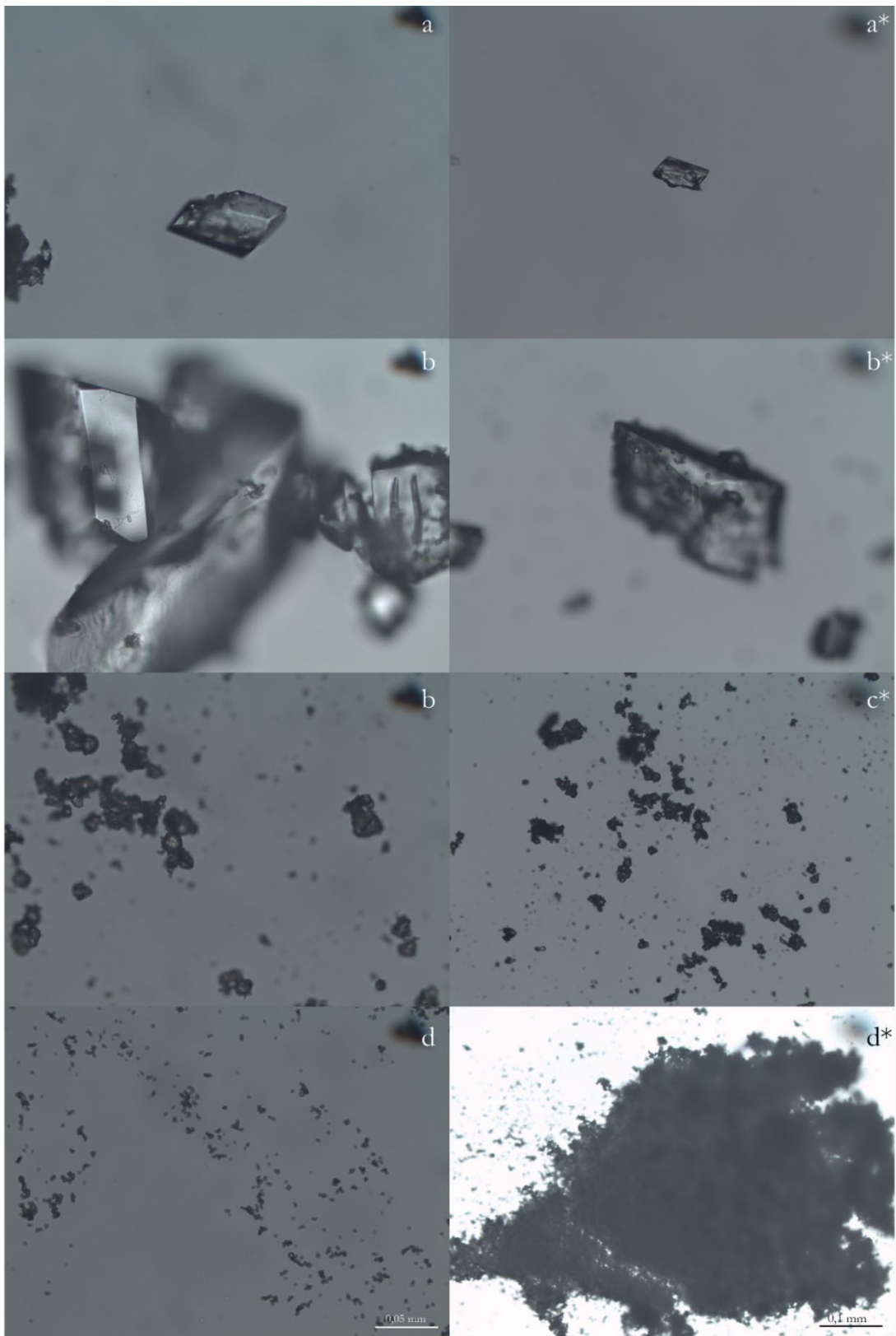


Figure 5 Images from the microscopy photographs, taken at Stockholm University Department of Geology. Using a Nikon microscope and Leica camera. The images on the left side and without a "*" are taken with a 40x magnification objective lens while images on the right side and marked with a "*" are taken with a 20x magnification objective lens. Scale markings at the bottom correspond to all images above. Images are taken from minerals from series 4 as in table 1.

4.2 ICP-OES analysis and PhreeqC simulation

4.2.1 ICP-OES Results

In the modeling, the results from the ICP-OES analysis were used to predict the saturation indices and pH for the resulting mixtures. In table 3, the result from the ICP-OES analysis can be seen. As with each mixture, the relative proportion of seawater is increasing, the results of the final analyses are expected to be close to those of seawater. As with each recycling more seawater is introduced including the main element of interest Ca. By comparing the seawater analysis with those of the experiments, it can be deduced that the final experiments are heavily depleted in Ca. This is based on the assumption that the experiments would be close to seawater in its measured values as the recycling is repeated. In table 2 the ratios of Ca and Mg in the liquid from the experiments to seawater are shown. The expected ratio was added

Table 2 In the table the results of the ICP-OES, table 3, are compared to the expected ratios if there was not precipitation. This was calculated by dividing the results by the average of the sea water results.

Experiment	Temp	Ca ratio	Mg ratio	Expected ratio
3-22-a	5°C	4%	52%	50%
3-22-b		8%	80%	75%
3-22-c		20%	100%	88%
3-22-d		45%	110%	94%
4-22-a	20°C	4%	51%	50%
4-22-b		7%	83%	75%
4-22-c		15%	103%	88%
4-22-d		37%	112%	94%
4-22-e		71%	114%	97%
6-22-a	5°C	4%	54%	50%
6-22-b		7%	82%	75%
6-22-c		20%	103%	88%
6-22-d		56%	108%	94%
5-22-a	20°C	4%	51%	50%
5-22-b		8%	87%	75%
5-22-c		16%	101%	88%
5-22-d		41%	107%	94%
5-22-e		73%	115%	97%

as a comparison to what ratio would be expected if no precipitation occurs. Thus, during the initial experiment where a mixture of 50% seawater and 50% are combined a ratio of about 50% Ca would be expected without precipitation. With each experiment the expectation is that the Ca will be bound into ikaite or other carbonate minerals. As can be seen in table 2 the Ca ratio at the initial experiment was 4% compared to the ~ 50% of Mg. Mg follows the expected ratio quite closely indicating little to no precipitation of Mg. Conversely the Ca ratio lies far from the hypothetical expected ratio. The initial experiment shows 4% while the first recycling shows a ratio of 8%. This trend continues for all the recycling experiments to a lesser degree. These results indicate that the resulting mixtures are lower in Ca than would be expected without precipitation.

Table 3 Results from the ICP-OES analysis in ppb. The results are accurate within 3-10%.

Experiment	Temp	Ca (ppb)	Mg (ppb)	Na (ppb)	S (ppb)	K (ppb)	Sr (ppb)	Al (ppb)
3-22-a	5°C	8 980	337 505	4581 538	203 073	118 483	442	325
3-22-b		16 961	521 786	5172 332	298 223	178 126	1 302	302
3-22-c		42 844	656 255	5686 298	361 545	223 053	2 262	333
3-22-d		95 488	717 991	5866 876	397 167	235 862	2 199	322
4-22-a	20°C	8 459	334 047	4677 922	198 678	117 108	538	313
4-22-b		14 214	546 875	5392 986	312 768	185 045	1 522	325
4-22-c		32 936	672 605	5914 018	373 389	227 757	1 005	357
4-22-d		78 763	733 932	6085 849	396 209	241 573	1 279	368
4-22-e		151 096	747 041	6078 038	404 433	251 904	2 714	328
6-22-a	5°C	9 416	351 426	4763 071	205 794	120 017	440	319
6-22-b		14 412	537 763	5294 804	313 028	187 669	1 113	934
6-22-c		43 019	674 483	5850 757	358 697	221 248	1 875	336
6-22-d		119 085	707 264	5832 746	389 757	236 060	2 960	375
5-22-a	20°C	8 962	331 007	4553 970	200 288	116 056	385	326
5-22-b		16 031	568 367	5569 247	301 119	187 946	689	304
5-22-c		35 207	660 443	5724 827	361 339	218 087	582	342
5-22-d		87 268	702 262	5949 457	389 478	242 073	1 406	374
5-22-e		155 066	754 859	5968 612	404 601	242 197	2 773	354
SW 1	N/A	219 120	678 301	5500 156	392 024	243 215	3 939	320
SW 2		208 330	632 360	5297 498	378 953	228 478	3 754	304
1:2 1	N/A	2 147	812	3932 794	N/A	N/A	N/A	408
1:2 2		1 824	578	3893 980	N/A	N/A	N/A	397
1:2 3		1 906	492	4006 463	N/A	N/A	N/A	379
1:2 4		1 975	521	3854 837	N/A	N/A	N/A	392

4.2.2 PhreeqC modelling results

PhreeqC was used to calculate SIs for the minerals that were precipitating during experiments performed by Stockmann et al., (2018) and Tollefsen et al., (2020). The identified minerals during these experiments were calcite, ikaite, vaterite, nesquehonite, aragonite and monohydrocalcite. The full results of the analyses are shown in the supplementary material (Appendix B). The saturation index of amorphous calcium carbonate has been excluded because it was not possible to identify within the scope of the study. As can be seen in figure 6, nesquehonite has a negative saturation index (SI) meaning that it is unlikely for this mineral to precipitate in the experiments. The other minerals all showed positive SI from highest to lowest order; calcite, aragonite, vaterite, monohydrocalcite and ikaite. Based purely on equilibrium thermodynamics, calcite is most likely to precipitate and ikaite is least likely.

The general trend is a reduction in the SI for all minerals identified at approximately the same intervals. It is interesting to note that SI for ikaite in the 20°C fourth recycling experiment drops to below 0. And from these results ikaite should not precipitate during the fifth recycling. For all series and minerals the index drops as the experimental series progresses. Indicating that for all

experiments precipitation becomes less likely. With the largest drop occurring between first (b) and second (c) recycling for the 5°C series. While for the 20°C the biggest drop occurs between third (d) and fourth (e) recycling for series 2 and the drop occurred over three recycling experiments from the second (c) to the fourth (e) recycling for series 4.

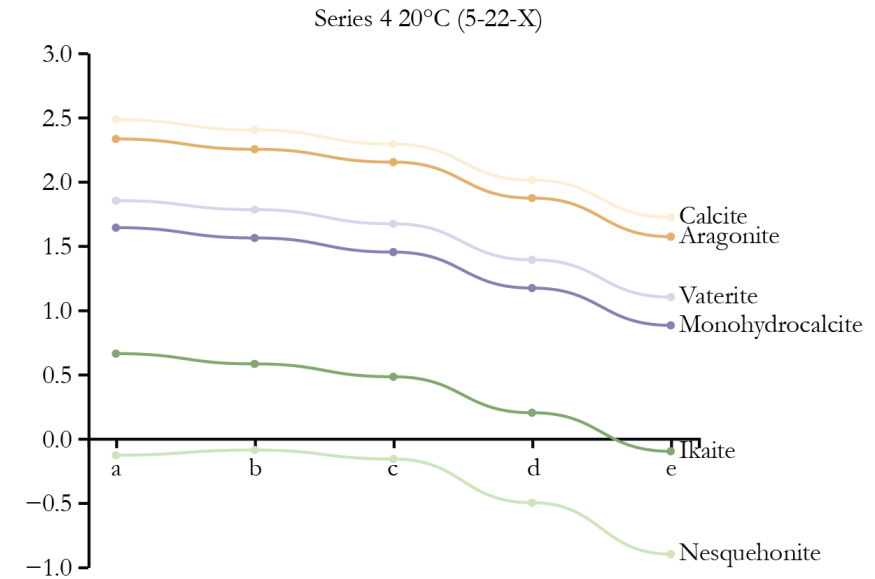
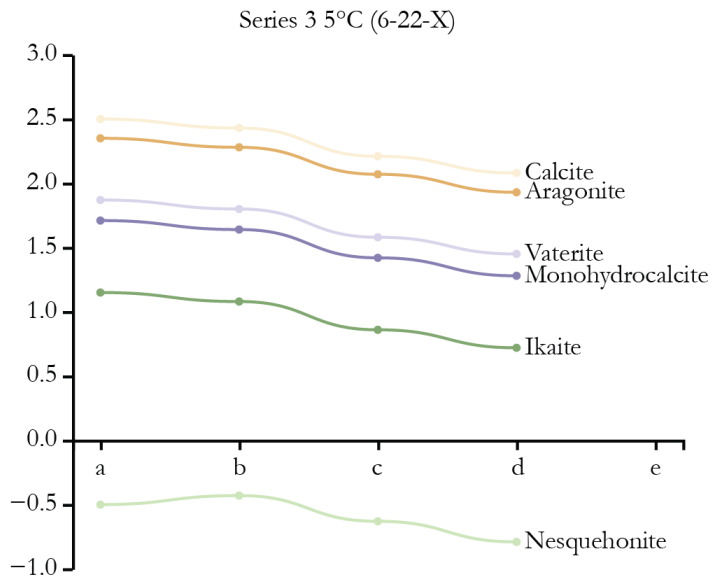
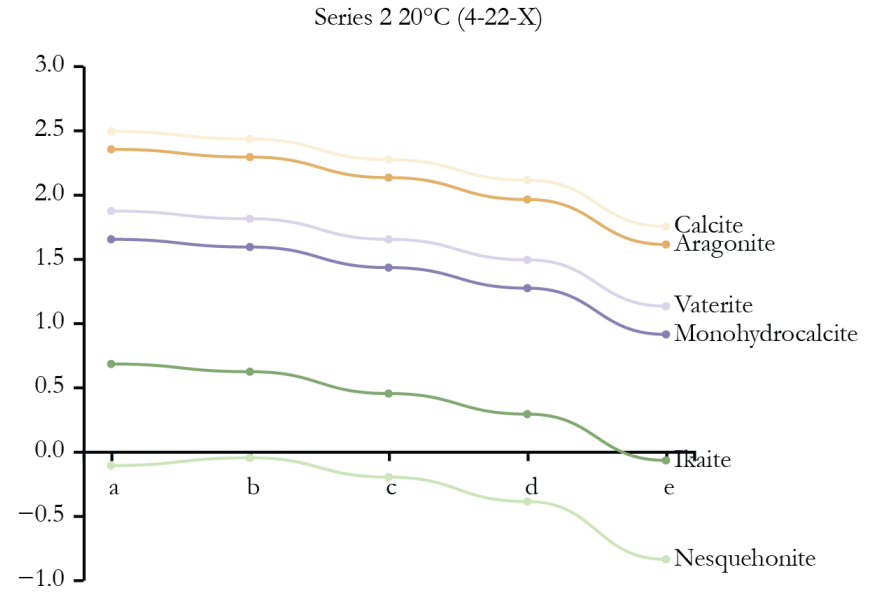
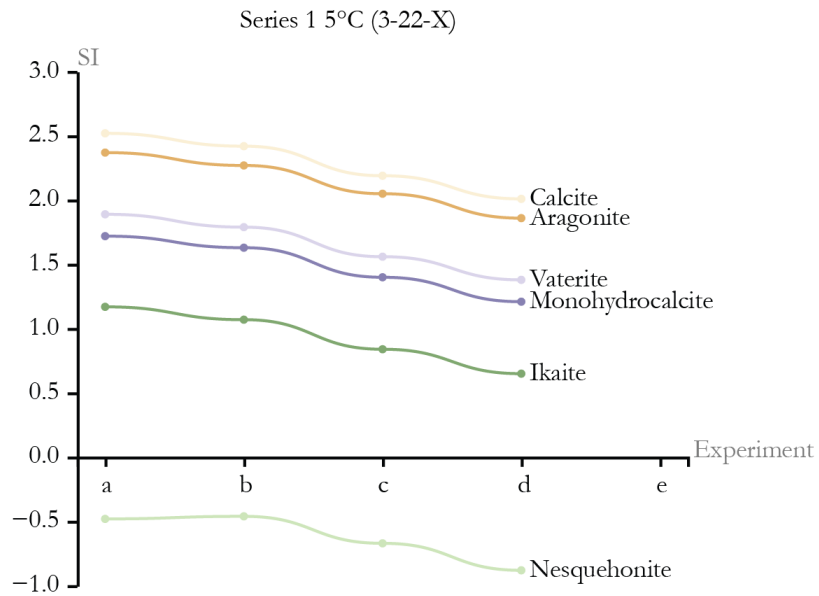


Figure 6 For the PhreeqC analysis the input was based on ICP-OES analysis data from the seawater and reactant fluid. Showing the saturation indices for theoretical mixtures of seawater with the residue from the experiments performed. Where a corresponds to the initial experiments and b with the first recycling, c the second, d the third and, e the fourth recycling.

4.3 PhreeqC pH modeling

Due to the complications in measuring pH noted in section 3.2, it was concluded that the pH measurements from the experiments would not be representative. As such the pH from the PhreeqC modeling was used. This will show the pH at the moment of mixing and thus incorporates all components. As indicated in table 4 in which the results of the experiments and the PhreeqC modelling are compared, the gap between the two methods becomes smaller as the experiment series progresses. In figure 6, pH calculated using PhreeqC has been plotted for each of the experimental runs. As can be seen the pH drops as the experiments progresses. However, the point of no precipitation is quite different between the two temperatures at which the experiments were performed at. In the 20°C series, a lower pH was reached than in the 5°C series. The pH for 5°C reached ~ 9.8, while at 20°C this was between 9.2 and 9.3. The drop between the third (d) and fourth (e) recycling for series 2 and 4 seems to only occur for those series. Thus, all the experiments show a steady drop in pH until the third recycling (d), after which only series 2 and 4 show a significant drop.

Table 4 Showing the comparison of the results from the experiments measurement and the PhreeqC modelling

Sample Name	pH experiment	pH PhreeqC	Difference
Series 1, 5°C			
Exp 3-22-a	10.41	10.24	0.17
Exp 3-22-b	10.09	9.99	0.10
Exp 3-22-c	9.85	9.75	0.10
Exp 3-22-d	9.49	9.44	0.05
Series 1, 20°C			
Exp 4-22-a	10.35	10.07	0.28
Exp 4-22-b	10.05	9.87	0.18
Exp 4-22-c	9.77	9.62	0.15
Exp 4-22-d	9.38	9.28	0.10
Exp 4-22-e	8.75	8.72	0.03
Series 1, 5°C			
Exp 6-22-a	10.44	10.25	0.19
Exp 6-22-b	10.11	10.00	0.11
Exp 6-22-c	9.85	9.76	0.09
Exp 6-22-d	9.52	9.47	0.05
Series 1, 20°C			
Exp 5-22-a	10.34	10.08	0.26
Exp 5-22-b	9.99	9.88	0.11
Exp 5-22-c	9.74	9.60	0.14
Exp 5-22-d	9.29	9.20	0.09
Exp 5-22-e	8.77	8.73	0.04

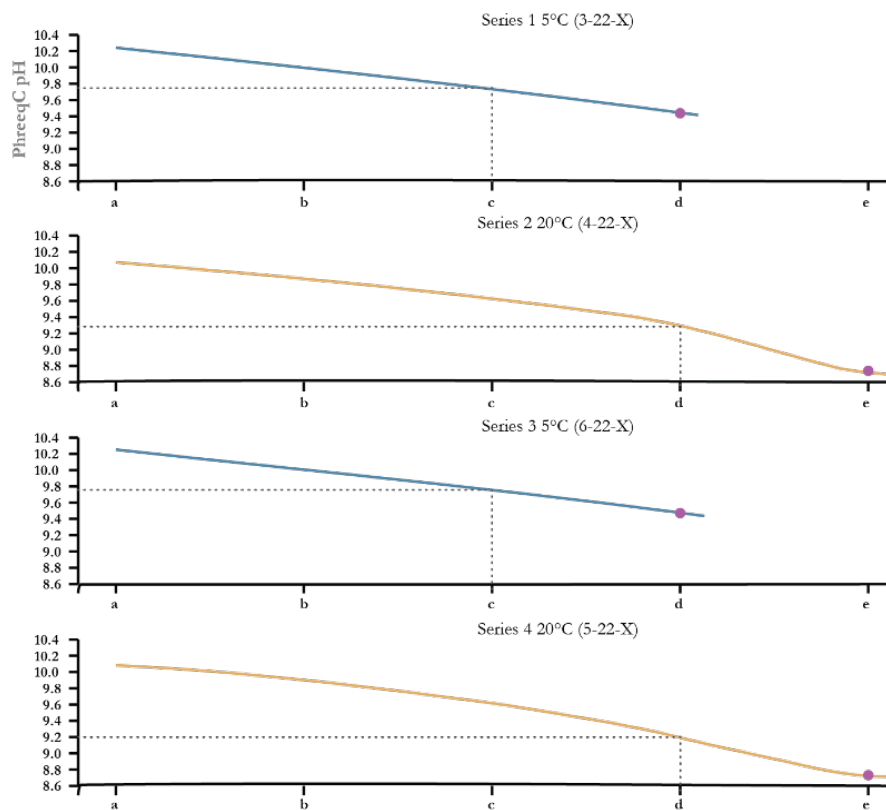


Figure 7 The graph above shows the pH progression through the experimental series. The dotted line indicates the cut off for precipitation. Purple dot indicates last experiment performed. Blue lines are indicative for 5°C and orange for 20°C.

4.3 XRD analysis

Table 5 shows the results of the XRD analysis with the use of Highscore. The percentages are approximate. The results can be further refined using Highscore, however this would result in changes of a few percent. Thus, for the scope of the study this has not been done. As it is not expected that the results will materially change if further refinement was to be applied. As can be seen in table 5, in all series ikaite formed during the first experiment and all precipitate was ikaite. The first recycling experiments precipitated only or for the most part ikaite. However, for the second recycling (c) experiments, deviations were observed. In the 5°C series, the amount of ikaite decreased and monohydrocalcite as well as smaller amounts of aragonite were observed. The 20°C series showed no ikaite in the second recycling (c) and instead saw a mix of monohydrocalcite and aragonite. In both occasions, the third recycling (d) precipitated aragonite only. Amorphous calcite was not found in any of the experimental runs.

Table 5 Below the results of the XRD analysis can be found. The XRD analysis has been performed at the Swedish Natural History Museum and the results have been analysed using Highscore and Rietvel refinement.

Name	Ikaite	Monohydrocalcite	Aragonite
Series 1, 5°C			
Exp 3-22-a	100%		
Exp 3-22-b	89%	11%	
Exp 3-22-c	37%	63%	
Series 2, 20°C			
Exp 4-22-a	100%		
Exp 4-22-b	88%	12%	
Exp 4-22-c		86%	14%
Exp 4-22-d			100%
Series 3, 5°C			
Exp 6-22-a	100%		
Exp 6-22-b	100%		
Exp 6-22-c	73%	18%	9%
Series 4, 20°C			
Exp 5-22-a	100%		
Exp 5-22-b	82%		18%
Exp 5-22-c		56%	44%
Exp 5-22-d			100%

5. Discussion

The discussion section is divided in two parts. In the first part, factors known to influence precipitation of ikaite will be discussed. These are temperature, pH and magnesium (Mg) concentration. In these sections, results from this study are compared with the results of previous studies. In the second part, the percentage of CO₂ sequestered using recycling is discussed and compared with earlier preliminary results by (Tollefsen, n.d.). Additionally, on the implications of the findings from this study for carbon capture and storage will be discussed in terms of benefits and limitations.

5.1 Potential causes for precipitation

Previous literature identified three main factors in the precipitation of ikaite. These are identified by Stockmann et al., (2018) and Tollefsen et al., (2020, 2018) as temperature, pH and magnesium

concentration as well as the role of calcium concentration as a factor affecting the precipitation amount and nucleation of ikaite. As noted in all experiments, calcite had the highest saturation index and was as such the most likely candidate to precipitate over other minerals, based solely on equilibrium thermodynamics. Nonetheless, it was found in the XRD analysis that ikaite and monohydrocalcite, both of which have an SI that is consistently lower than calcite, preferentially precipitated in most experiments.

5.1.1 The influence of temperature on the precipitation of Ikaite

The influence of temperature on the precipitation of ikaite was long thought to be a major factor. However, more recent research showed that ikaite readily precipitates at higher temperatures as well as lower ones. The experiments performed at 5°C and 20°C provide a limited insight into temperature as a precipitation control of ikaite. The main benefit of running these two specific temperature series is to determine which allows for more yield/CO₂ sequestration. The run temperature of 5°C was chosen because it has been seen as to be within the ideal temperature range for ikaite precipitation (Bischoff et al., 1993a; Kawano et al., 2009; Marland, 1975; Shahar et al., 2005). The run temperature of 20°C was chosen to provide insights about ikaite precipitation at room temperature.

In the initial experiments, using the synthetic spring water mixed with seawater, ikaite always accounted for the full precipitate. This seems to affirm the earlier made remark that temperature indeed does not affect the precipitation of ikaite. When the reaction liquid is recycled and mixed with seawater, the pattern of which minerals precipitate changes. The XRD results show that other minerals than ikaite also precipitate. Ikaite precipitates for more recycling cycles at 5°C than at 20°C. This claim is also supported by the PhreeqC analysis where the SI index for ikaite remains higher at 5°C than at 20°C. This outcome suggests that during recycling, temperature does affect the precipitation of ikaite, with more precipitation at the lower temperature. However, it is important to note that in the 20°C recycling, the minerals monohydrocalcite and aragonite precipitate. Moreover, in the first experiment in which seawater is mixed with the synthetic spring water, only ikaite precipitates. Nevertheless, when the reaction fluid is recycled, ikaite precipitates more readily in the 5°C experiments.

5.1.2 The pH regime under which ikaite precipitates.

Apart from temperature, an important influence is pH. For the precipitation of ikaite from natural seawater, a pH of 9.3 or higher is required (Tollefsen et al., 2018). The results from the experiments

are in line with this premise in which precipitation of ikaite only happened at a pH higher than 9.3. Figure 8 and 9 show precipitation as a function of pH and magnesium concentration. The figures show that when the pH drops below 10, monohydrocalcite and aragonite start precipitating in addition to ikaite at 5°C or instead of ikaite at 20°C. Coincidentally, the pH drops below 10 when recycling, marked b and onwards, is applied to the experiments. The difference between the 5°C and 20°C experiments lie in the point at which no precipitation occurs. In the 20°C experiments the point at which no precipitation no longer occurs is around the pH 9.3. But, for the 5°C experiments this point is around pH 9.7. Indicating that the temperature enhances precipitation even though it is not ikaite. However, the PhreeqC analysis shows that precipitation is possible based on the SI indices. These results indicate that a high pH environment is crucial in order for precipitate to form, with the lowest at which ikaite forms being pH 9.8 at 5°C and pH 9.9 at 20°C. Concurrently, other minerals such as monohydrocalcite and aragonite precipitate. The fact the pH decreases with each recycling sets a limit to the number of cycles after which ikaite will precipitate.

5.1.3 Magnesium and its role as an inhibitor of calcite growth

As has been observed in the results from the PhreeqC modelling, the saturation index of calcite is higher than that of the other observed minerals. In previous literature on the topic, it has been suggested that magnesium acts as a calcite growth inhibitor. For the precipitation of ikaite, the mixture of seawater and spring water needs a Mg concentration of 22.8 ± 0.50 mmol/kg and a pH 9.3, (Tollefsen et al., 2018). The seawater used in the experiments had a of Mg concentration of 27 ± 1.90 mmol/kg, which results in an approximate Mg concentration of 14 mmol/kg in the initial experiment. See figure 8 and 9. This leads to a much lower Mg concentration than in earlier experiments with a higher pH value. However, during the recycling stage, the Mg concentration is up to 22 mmol/kg. As there have been no instances of calcite precipitation, neither during the initial experiment nor during the recycling stage, it is likely that magnesium acted as an inhibitor to the precipitation of calcite, even at the lower concentration in the initial experiment

Table 6 The table above shows the results from the ICP-OES analysis over Styrsö seawater. The concentrations

	mmol/kg	mmol/kg
Ca	5.5	5.2
K	6.2	5.8
Mg	27.9	26.0
Na	239.2	230.4
S	12.2	11.8

Precipitate as a function of magnesium and pH

The results from two series can be seen below. X represents series three and X' series four. The graph below shows on the X axis the Mg content in mmol/kg from the ICP-OES measurement, and the Y axis shows the pH as modelled in the PhreeqC software. The circle size shows the amount of g/kg precipitate obtained from the experiments. The color of the circle indicates the temperature of the experimental series. The doughnut chart overlaying the circle shows the results from the XRD measurements. The specific meaning of the colors can be seen in the legend to the right. The graph was plotted using RAW graphs and edited in Adobe Illustrator.

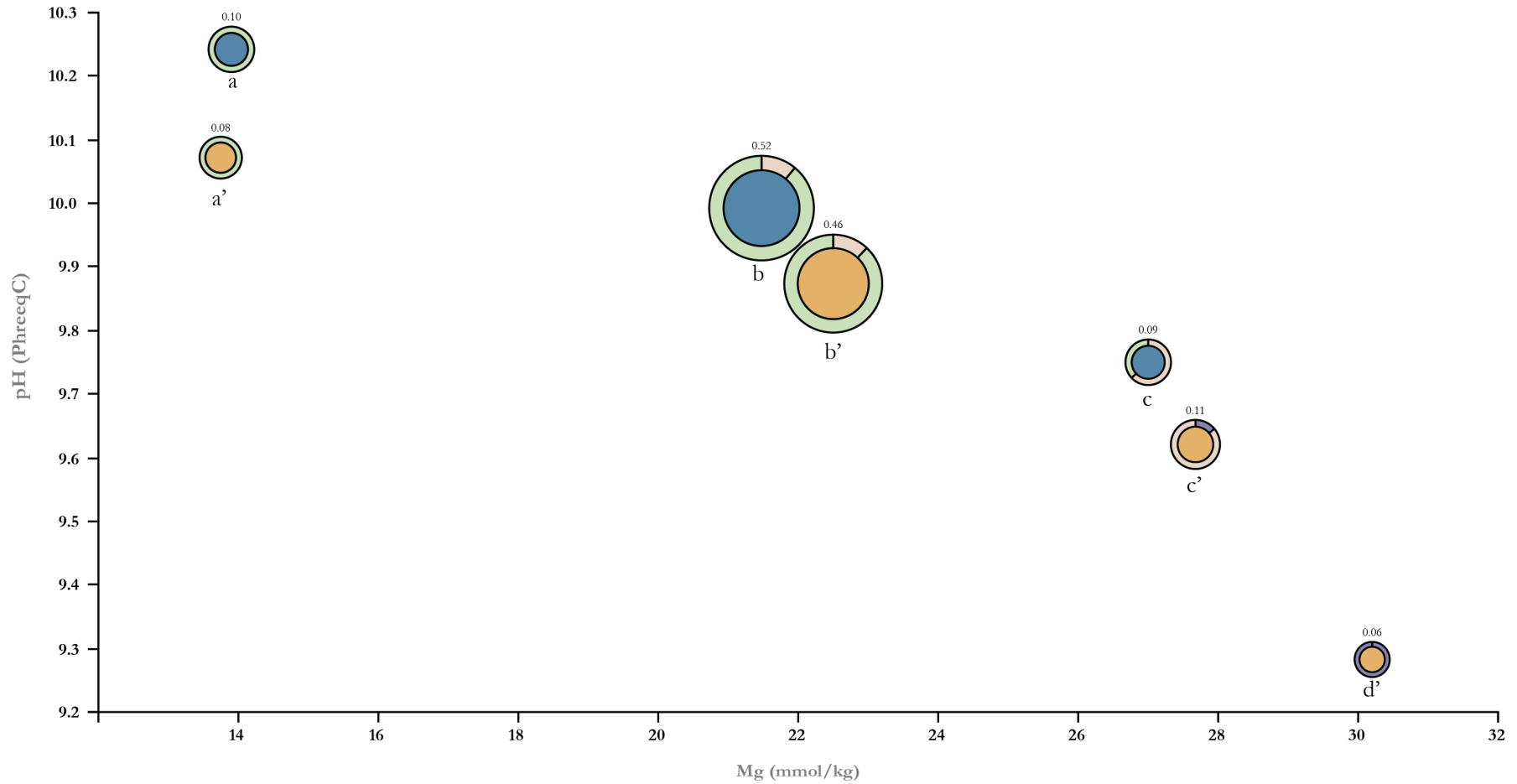
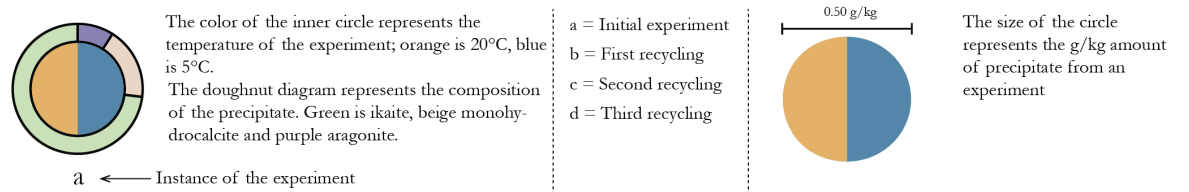


Figure 8 Main results figure combining the results from the experiments, ICP-OES, PhreeqC and XRD in one graph.

Precipitate as a function of magnesium and pH

The results from two series can be seen below. X represents series six and X' series five. The graph below shows on the X axis the Mg content in mmol/kg from the ICP-OES measurement, and the Y axis shows the pH as modelled in the PhreeqC software. The circle size shows the amount of g/kg precipitate obtained from the experiments. The color of the circle indicates the temperature of the experimental series. The doughnut chart overlaying the circle shows the results from the XRD measurements. The specific meaning of the colors can be seen in the legend to the right. The graph was plotted using RAW graphs and edited in Adobe Illustrator.

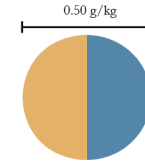


The color of the inner circle represents the temperature of the experiment; orange is 20°C, blue is 5°C.

The doughnut diagram represents the composition of the precipitate. Green is ikaite, beige monohydrocalcite and purple aragonite.

a ← Instance of the experiment

- a = Initial experiment
- b = First recycling
- c = Second recycling
- d = Third recycling



The size of the circle represents the g/kg amount of precipitate from an experiment

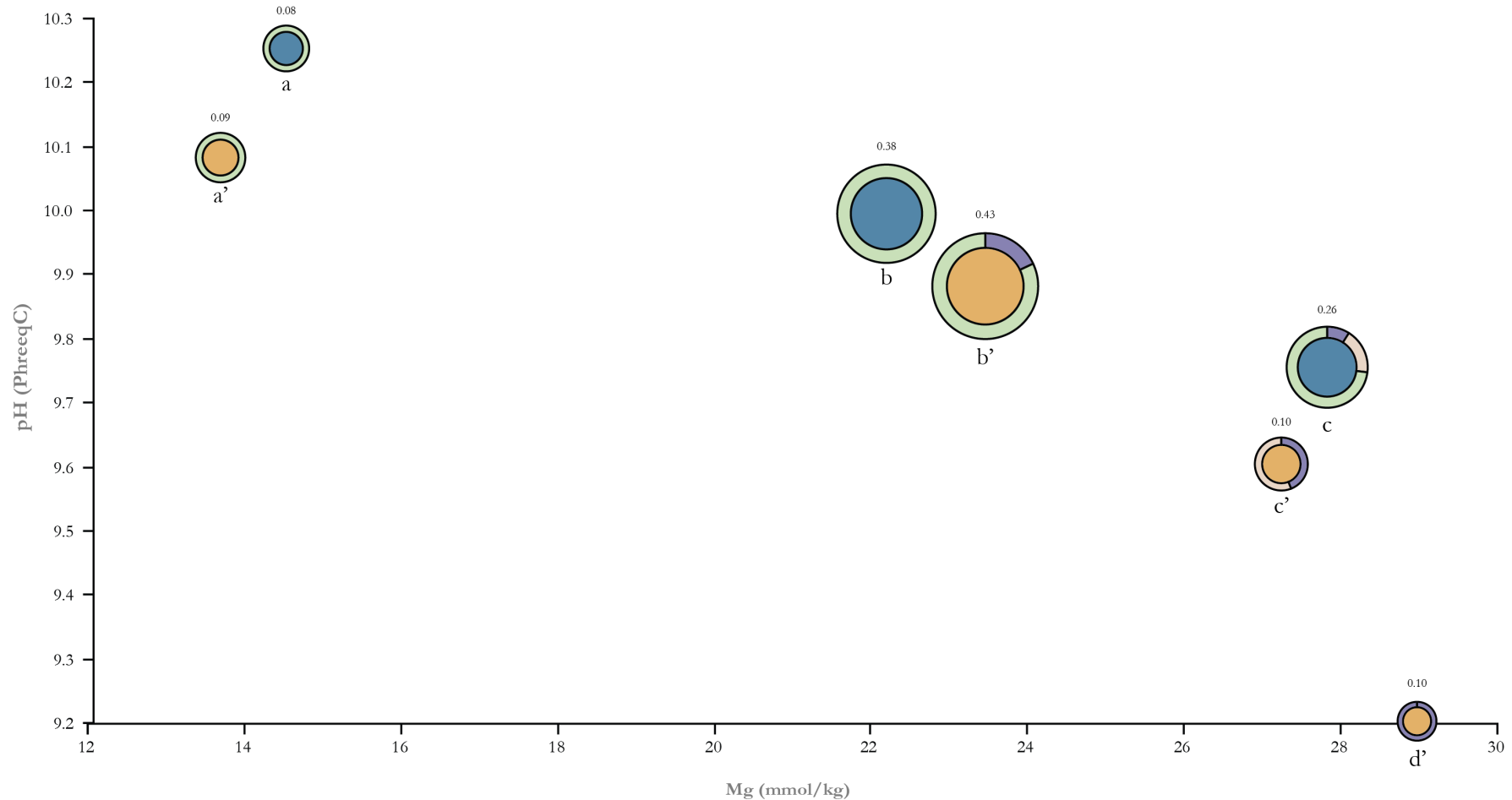


Figure 9 Main results figure combining the results from the experiments, ICP-OES, PhreeqC and XRD in one graph.

5.1.4 Alternative explanations to precipitation patterns

As was noted in the results, the largest g/kg precipitation occurred in the first recycling for all experiments, marked b and b' in figure 8 and 9. Where g/kg is the amount (g) of precipitate precipitated per kilogram (kg) of reactant fluid. However, as can be seen in figure 10 below, in both the initial (“a”) and the first recycling (“b”) the residual fluid is low in Ca, compared to the seawater. As the input for both these instances of Ca is approximately equal, the output should also be comparable. Thus, as they are not comparable, there ought to be another explanation for the pattern observed. One of the observations made during the experiments, and in particular during the filtering stage, was that the residual fluid was still lightly clouded after filtering of the initial experiment. This was interpreted to mean that the filter used, the Munktell 00K, was not fine enough to capture all precipitate and let some through. As such, the results seem to indicate that this has caused some carry over effect. This means that particles that have precipitated in the initial experiment are present during the next experiment.

If the aforementioned theory is correct, some of the precipitate of the initial experiment is used in the first recycling experiment. There would be a two-fold effect from this. Firstly, that some of the precipitate is transferred from the first experiment to the second experiment, thus increasing the weight. When estimating the impact of this, the following errors should be taken into consideration; some of the precipitate will remain on the filter, ICP-OES measurements are not 100% accurate and any human errors made in the handling and testing of the samples. Assuming that none of these errors occurred, approximately 0.4g/kg precipitate is missing from the initial experiment. This would suggest that 0.4g/kg is introduced from the initial experiments into the recycling stage. This calculation assumes that only ikaite precipitates, which is heaviest among the minerals observed to precipitate during the experiments. However, the recalculation of the recycling stage does not suggest that the full amount is carried over, which achieves approximate full precipitation with the input of calcium (see appendix C for full data and calculation). Thus, based on the available data, it is likely that a proportion of the precipitate is introduced from the initial stage into the recycling stage. Secondly, the prior particles would offer nucleation points for further precipitation in the recycling stage. This would create fewer larger crystal to form from the solution, and possibly lower the kinetic barrier for precipitation. The observation that the filtered fluid was clear after the second recycling seems to support the hypothesis that larger crystals formed. And is also seen in figure 5 where the largest crystals are observed in the first recycling. Thus, the two main hypotheses for seeing the most precipitate in the first recycling is that some of the precipitate of the initial experiment has been introduced in the first recycling. And that due

to the introduced nuclei the precipitation in the first recycling was more efficient, creating larger crystals and more efficient collection.

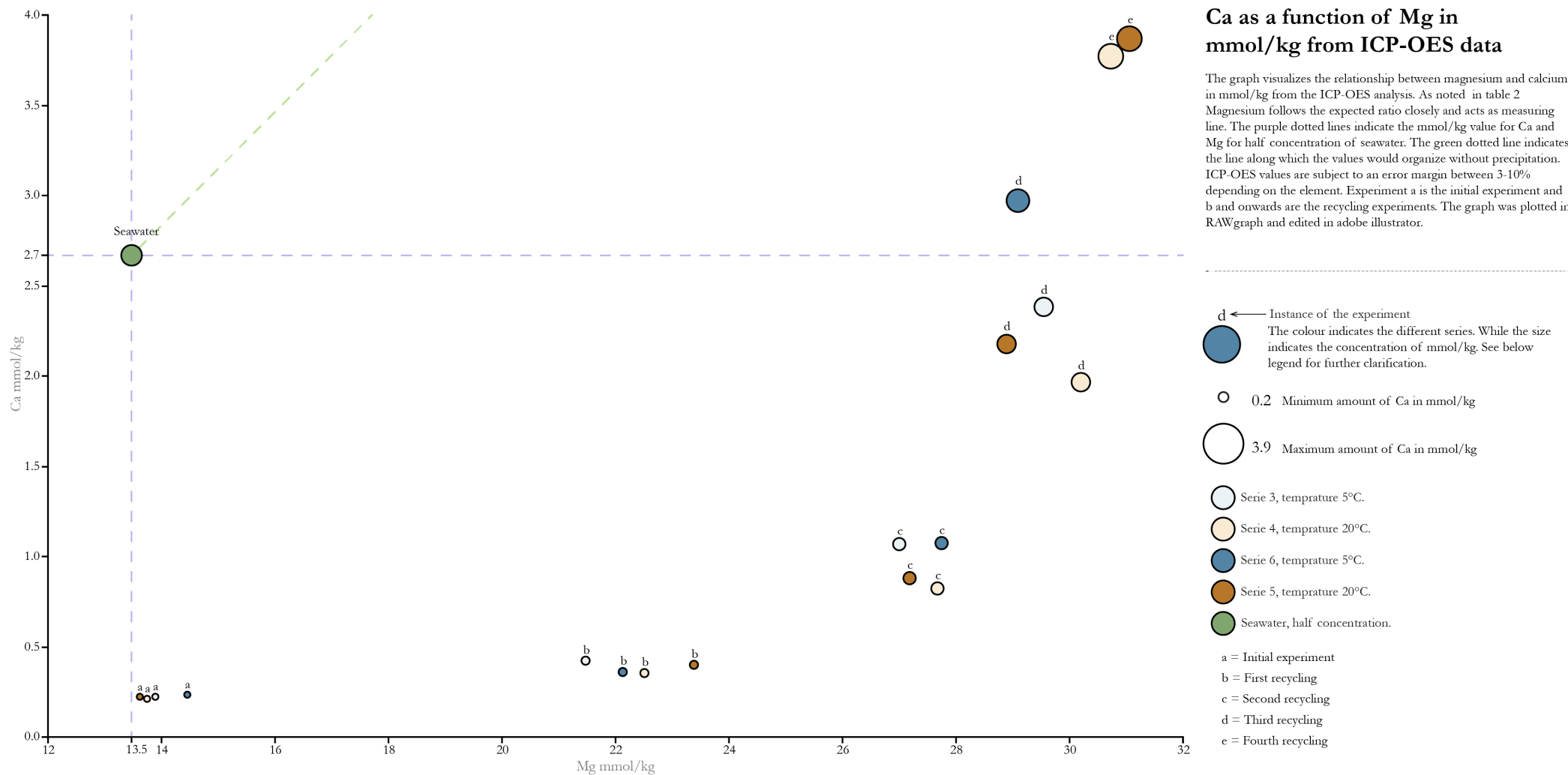


Figure 10 The figure shows the relationship between the mmol/kg concentrations of Mg and Ca. Included is the half concentration of seawater with all data obtained from ICP-OES analysis of residual water.

5.2 Ikaite precipitation in comparison with other CCS methods

This section has two parts. In the first part, the amount of CO₂ sequestered at each stage of the experiment will be discussed as will the potential limitations of this approach. In the second part, the results from the first part will be compared against two other CCS methods highlighting limitations and benefits in the employed method.

5.2.1 Percentage of CO₂ sequestered.

The approximate percentage of CO₂ sequestered can be calculated by combining the results from the experiments with the results from the XRD analysis. Figure 11 shows the visualization of this calculation. In the figure below, series 1 and 3 correspond to the experiments performed at 5°C while 2 and 4 correspond to those at 20°C. As can be seen in both, the first set of experiments and the duplicates yield similar results. At 5°C, 4% and 3.9% of the CO₂ is sequestered in series 1 and 3, after completion of all experiments. At 20°C, 4.6% and 4.7% of the CO₂ is sequestered in series 2 and 4. Importantly, figure 11 demonstrates clearly that most of the CO₂ is sequestered in the recycling stage of the experiments. The initial run sequesters around 0.4-0.5% of the CO₂, whereas around 1.9-2.8% is sequestered in the first recycling.

In addition to the possible causes for more sequestration occurring during recycling which were discussed in section 5.1.4., another consideration is that the lower amount of sequestering in the first experiment might be due to the chemistry of the seawater. When comparing the seawater used in the experiments to the seawater used in earlier experiments the Ca concentration is between 5.5 and 5.2 mmol/kg, see table 6, while Tollefsen et al., (2018) used seawater with 8.82 ± 0.22 mmol/kg. Indicating that the seawater used in the experiments is possible not collected in the correct way. And as such it might be mixed with fresh water or other sources of decreasing the salinity. However, as their study was not centered around sequestration, no direct comparison can be made. Nevertheless, both experimental set ups used 50% seawater and 50% of carbonate mixture. Thus, by the first recycling in this study, more Ca was introduced than in those experiments. A further limitation is from the collection of precipitate, as noted earlier the weights are affected by the effectiveness of the scraping from the filter paper. In this process there is always a portion of the precipitate that remains behind. As such, the weight will be underestimated. An additional limitation is that the peristaltic pump did not always give the same output despite having the same set up. This may have influenced the amount of CO₂ and Ca²⁺ introduced into the

mixture. Nevertheless, because continued recycling was applied, this is unlikely to have been a constraint.

Taking these constraints into account, the results of this study suggest that recycling the solution allows for more sequestering of CO₂. Compared with the results achieved in (Tollefsen, n.d.), which achieved ~2% sequestering, the results show that recycling allows for additional CO₂ to be sequestered.

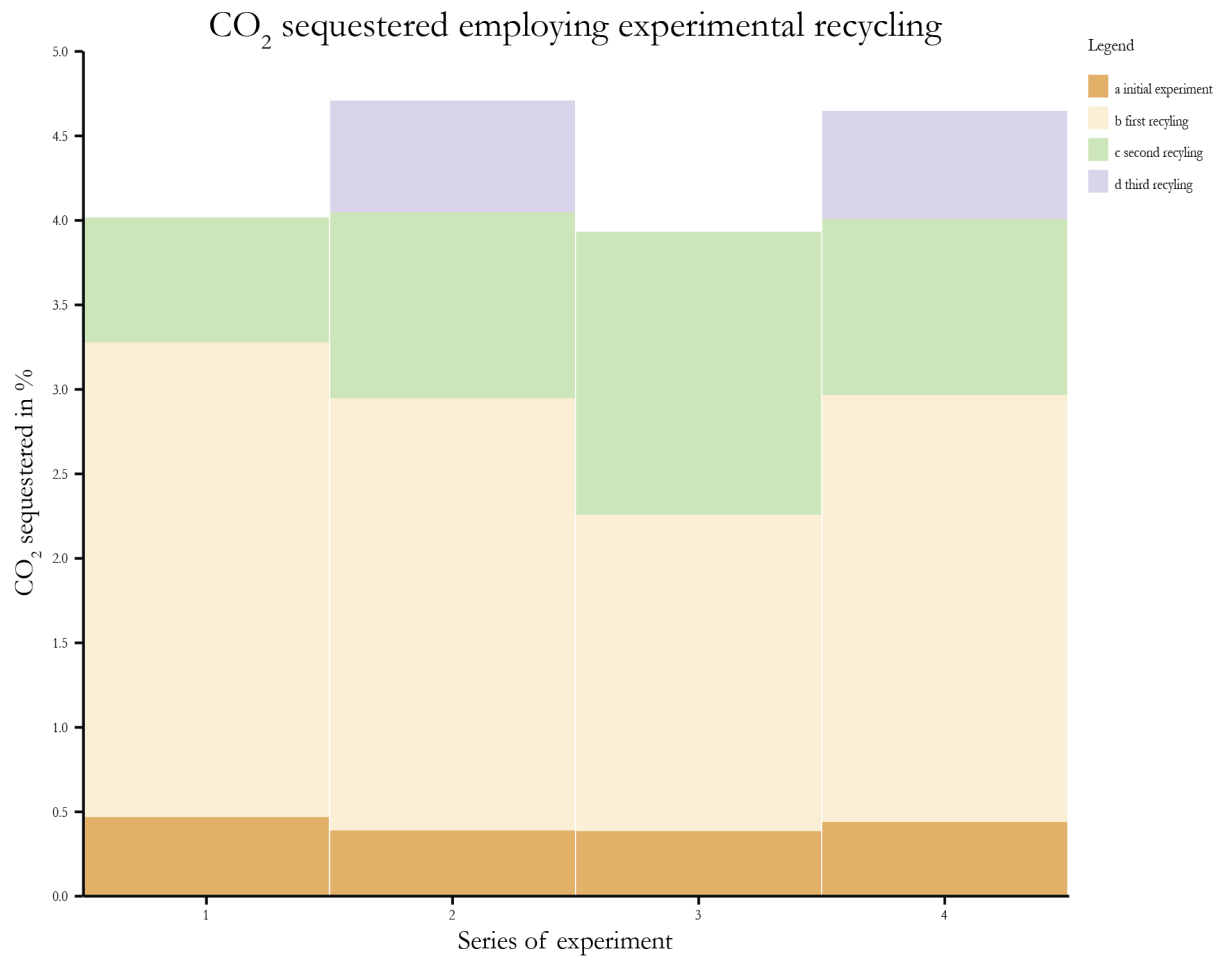


Figure 11 The graph shows the results in % of CO₂ introduced into the mixture. In the graph the dark orange colour shows the initial experiment which used the carbonate mixture. After which the results from the recycling stages are shown. Series 1 and 2 are the initial experiments which were performed at 5°C and 20°C while series 3 and 4 are duplicates. The supporting material can be found in appendix D.

5.2.2 Comparison to other CCS methods

The CCS method with ikaite will be compared with two other methods that are being used at the moment. The first is the storage of CO₂ into subsurface sedimentary basins. The second is the project in Iceland named CarbFix, which pumps CO₂ into basaltic layers.

The first method, of pumping CO₂ directly into sedimentary basins, has the advantage that large amounts can be pumped into the sedimentary basin. However, in comparison to the method using ikaite there are two major drawbacks. The first is that, because CO₂ is stored as a liquid, there is a risk that, due to for instance earthquakes, the CO₂ starts leaking out. Additionally, in order for this method to work it needs a specific geological location in the form of sedimentary basins. This comes with the added downside that CO₂ will have to be transported to suitable sites. Thus, the limiting factors in this method are the risk of leakage, and the need for a specific locality to employ the method.

The method used in Iceland results in the sequestering of CO₂ as minerals and research has shown that within two years nearly complete in situ CO₂ mineralization occurred (Gislason and Oelkers, 2014; Matter et al., 2016). The main advantage is the near complete and relatively fast mineralization of the CO₂ injected. This method also has the downside that it requires specific geology in order to be used. Specifically, mafic rocks, such as basalts, are required as these react with dissolved CO₂. These are relatively abundant but are not necessarily near the sources of CO₂. In comparison to the less than two years taken for sequestration in Iceland, sequestration of CO₂ as ikaite took approximately 96 hours for 4.5% sequestration of CO₂. Therefore, CarbFix is limited in terms of locations as well as being slower. On the other side it has a major advantage with the near complete sequestering of CO₂.

The ikaite method has advantages in terms of timescale and applicability in comparison with the other two methods. As the main component needed for this method is CO₂ and seawater, it can be used close to the source of CO₂. Another advantage is the speed with which the reaction occurs, which is a matter of days rather than years. The main downside is the relatively low percentage of sequestration.

6. Conclusion

6.1 Concluding remarks.

The aim of the study was to figure out whether recycling the solution from which ikaite precipitates increases the yield. The results obtained confirm that the yield does increase when the solution is recycled with more seawater. This was shown in the amount of precipitate obtained, where the first recycling yielded the most ikaite. It was noted that as the reaction continued, other minerals also started precipitating, which was in the form of monohydrocalcite

and aragonite. The experiments sequestered more CO₂ than was obtained during pilot study into ikaite as an intermediary for CCS. With up to 4.6% of the CO₂ compared to the ~ 2% of the initial study. It was noted that the experiments performed at 20°C sequestered more CO₂ than the experiments at 5°C, sequestering ~4.5% and ~4% respectively. Thus, recycling the solution from which ikaite precipitates increases the yield.

6.2 Limitations and further research

The following limitations were encountered during the performance of the experiments. First and foremost, the seawater collected was likely mixed with surface water. This became apparent from the ICP-OES analysis as the components were rather low in comparison to seawater tested in earlier experiments. This has possibly affected the yields in a negative manner. Moreover, there were issues with obtaining all the precipitate. Especially with the precipitate, it is not always possible to acquire everything from the beaker it precipitates in. Nor it is possible to scrape the filter paper perfectly clean. Another concern is that the liquid that is recycled into the next experiment continues the precipitate in the container it is stored in, before being used again. All these limitations impact the yield negatively, taking some of the precipitate out of the equation.

There are additional errors that may occur during the weighing and processing of data, these are combined into the human error. As the data is recorded, processed and used, there is always a chance that a mistake was made that influences the results was overlooked.

Lastly, the machine errors must be taken into account. As there was a wide array of methods employed in this thesis, the focus will be on the main three components; the XRD, ICP-OES and PhreeqC software. In each of these, there is potential for errors occurring. While highly accurate, the XRD still required human input for identification of minerals, and, as noted earlier, only the approximate percentages were obtained due to time limitations. In the ICP-OES errors may have occurred during the preparation of the samples. Furthermore, an error possibly occurred within the measurements of the machine. The two seawater samples diverge slightly, even though the seawater was collected in the same location. The PhreeqC model also relies in part on the constraints and inputs of humans, as well as input from the ICP-OES measurements. As such there are many ways in which errors may occur while handling these machines and programs.

Finally, ideas for further research include studying the potential role of nuclei in the precipitation of ikaite. As was observed, these were introduced into the first recycling, which saw the highest

yield. Additionally, research into increasing the Ca^{2+} concentration in the initial experiment is recommended, to see if this increases yield. The incentive for this is that the Ca^{2+} remaining after the first two experiments was very low. Another possible line of research is to look further into increasing the pH during the experiments. The results of the present research showed that the saturation indexes were still high, while no further precipitation occurred. And lastly, experiments into the scalability of the process should be conducted in order to determine the best method for scaling up the operation.

Bibliography

- Alderton, D., 2021. Carbonates (Ca, Mg, Fe, Mn), in: *Encyclopedia of Geology*. Elsevier, pp. 382–394. <https://doi.org/10.1016/B978-0-08-102908-4.00088-6>
- Bischoff, J.L., Fitzpatrick, J.A., Rosenbauer, R.J., 1993a. The solubility and stabilization of ikaite ($\text{CaCO}_3 \cdot 6\text{H}_2\text{O}$) from 0° to 25°C : Environmental and paleoclimatic implications for thinolite tufa. *J. Geol.* 101, 21–33.
- Bischoff, J.L., Stine, S., Rosenbauer, R.J., Fitzpatrick, J.A., Stafford Jr, T.W., 1993b. Ikaite precipitation by mixing of shoreline springs and lake water, Mono Lake, California, USA. *Geochim. Cosmochim. Acta* 57, 3855–3865.
- Brečević, L., Nielsen, A.E., 1989. Solubility of amorphous calcium carbonate. *J. Cryst. Growth* 98, 504–510. [https://doi.org/10.1016/0022-0248\(89\)90168-1](https://doi.org/10.1016/0022-0248(89)90168-1)
- Buchardt, B., Israelson, C., Seaman, P., Stockmann, G., 2001. Ikaite tufa towers in Ikka Fjord, southwest Greenland: Their formation by mixing of seawater and alkaline spring water. *J. Sediment. Res.* 71, 176–189. <https://doi.org/10.1306/042800710176>
- Chang, R., Kim, S., Lee, S., Choi, S., Kim, M., Park, Y., 2017. Calcium carbonate precipitation for CO_2 storage and utilization: A review of the carbonate crystallization and polymorphism. *Front. Energy Res.* 5, 17. <https://doi.org/10.3389/fenrg.2017.00017>
- Chen, J., Xiang, L., 2009. Controllable synthesis of calcium carbonate polymorphs at different temperatures. *Powder Technol.* 189, 64–69. <https://doi.org/10.1016/j.powtec.2008.06.004>
- Degen, T., Sadki, M., Bron, E., König, U., Nénert, G., 2014. The HighScore suite. *Powder Diffr.* 29, S13–S18. <https://doi.org/10.1017/S0885715614000840>
- Dickens, B., Brown, W.E., 1970. The crystal structure of calcium carbonate hexahydrate at about -120°C . *Inorg. Chem.* 9, 480–486. <https://doi.org/10.1021/ic50085a010>
- Dieckmann, G.S., Nehrke, G., Papadimitriou, S., Göttlicher, J., Steininger, R., Kennedy, H., Wolf-Gladrow, D., Thomas, D.N., 2008. Calcium carbonate as ikaite crystals in Antarctic sea ice. *Geophys. Res. Lett.* 35, L08501. <https://doi.org/10.1029/2008GL033540>
- Dieckmann, G.S., Nehrke, G., Uhlig, C., Göttlicher, J., Gerland, S., Granskog, M.A., Thomas, D.N., 2010. Brief communication: Ikaite ($\text{CaCO}_3 \cdot 6\text{H}_2\text{O}$) discovered in Arctic sea ice. *The Cryosphere* 4, 227–230. <https://doi.org/10.5194/tc-4-227-2010>
- Falkowski, P., Hogberg, P., Seitzinger, S., Smetacek, V., Steffen, W., Scholes, R.J., Boyle, E., Candell, J., Canfield, D., Elser, J., Gruber, N., Hibbard, K., Linder, S., Mackenzie, F.T., Moore III, B., Pedersen, T., Rosenthal, Y., 2000. The global carbon cycle: A test of our knowledge of earth as a system. *Am. Assoc. Adv. Sci.* 5490, 291–296.
- Gebauer, D., Völkel, A., Cölfen, H., 2008. Stable prenucleation calcium carbonate clusters. *Science* 322, 1819–1822. <https://doi.org/10.1126/science.1164271>
- Gislason, S.R., Oelkers, E.H., 2014. Carbon storage in basalt. *Science* 344, 373–374. <https://doi.org/10.1126/science.1250828>
- Gopi, S., Subramanian, V.K., Palanisamy, K., 2013. Aragonite–calcite–vaterite: A temperature influenced sequential polymorphic transformation of CaCO_3 in the presence of DTPA. *Mater. Res. Bull.* 48, 1906–1912. <https://doi.org/10.1016/j.materresbull.2013.01.048>
- Gutjahr, A., Dabringhaus, H., Lacmann, R., 1996. Studies of the growth and dissolution kinetics of the CaCO_3 polymorphs calcite and aragonite II. The influence of divalent cation additives on the growth and dissolution rates. *J. Cryst. Growth* 158, 310–315. [https://doi.org/10.1016/0022-0248\(95\)00447-5](https://doi.org/10.1016/0022-0248(95)00447-5)
- Gutknecht, V., Snæbjörnsdóttir, S.Ó., Sigfússon, B., Aradóttir, E.S., Charles, L., 2018. Creating a carbon dioxide removal solution by combining rapid mineralization of CO_2 with direct air capture. *Energy Procedia* 146, 129–134. <https://doi.org/10.1016/j.egypro.2018.07.017>
- Hansen, M.O., Buchardt, B., Kuhl, M., Elberling, B., 2011. The fate of the submarine ikaite tufa columns in southwest Greenland under changing climate conditions. *J. Sediment. Res.* 81, 553–561. <https://doi.org/10.2110/jsr.2011.50>
- Hazen, R.M., Downs, R.T., Jones, A.P., Kah, L., 2013. Carbon mineralogy and crystal chemistry. *Rev. Mineral. Geochem.* 75, 7–46. <https://doi.org/10.2138/rmg.2013.75.2>
- Hesse, K.F., Koppers, H., Suess, E., 1983. Refinement of the structure of ikaite, $\text{CaCO}_3 \cdot 6\text{H}_2\text{O}$. *Z. Krist.* 163, 227–231.

- IPCC special report on carbon dioxide capture and storage, 2005. . Cambridge University Press, for the Intergovernmental Panel on Climate Change, Cambridge.
- Jones, A.P., Genge, M., Carmody, L., 2013. Carbonate melts and carbonatites. *Rev. Mineral. Geochem.* 75, 289–322. <https://doi.org/10.2138/rmg.2013.75.10>
- Kawano, J., Shimobayashi, N., Miyake, A., Kitamura, M., 2009. Precipitation diagram of calcium carbonate polymorphs: its construction and significance. *J. Phys. Condens. Matter* 21, 425102. <https://doi.org/10.1088/0953-8984/21/42/425102>
- Kintisch, E., 2016. New solution to carbon pollution? *Science* 352, 1262–1263. <https://doi.org/10.1126/science.352.6291.1262>
- Lane, J., Greig, C., Garnett, A., 2021. Uncertain storage prospects create a conundrum for carbon capture and storage ambitions. *Nat. Clim. Change* 11, 925–936. <https://doi.org/10.1038/s41558-021-01175-7>
- Marland, G., 1975. The stability of $\text{CaCO}_3 \cdot 6\text{H}_2\text{O}$ (ikaite). *Geochim. EtCosmochimica Acta* 39, 83–91.
- Matter, J.M., Stute, M., Snæbjörnsdóttir, S.Ó., Oelkers, E.H., Gislason, S.R., Aradóttir, E.S., Sigfusson, B., Gunnarsson, I., Sigurdardóttir, H., Gunnlaugsson, E., Axelsson, G., Alfredsson, H.A., Wolff-Boenisch, D., Mesfin, K., Taya, D.F. de la R., Hall, J., Dideriksen, K., Broecker, W.S., 2016. Rapid carbon mineralization for permanent disposal of anthropogenic carbon dioxide emissions. *Science* 352, 1312–1314. <https://doi.org/10.1126/science.aad8132>
- Mindat, Calcite [WWW Document], n.d. URL <https://www.mindat.org/min-859.html> (accessed 10.9.22).
- Pauly, H., 1963. “Ikaite”, a new mineral from Greenland. *Actic* 16, 263–264. <https://doi.org/10.14430/arctic3545>
- Plummer, L.N., Busenberg, E., 1982. The solubilities of calcite, aragonite and vaterite in $\text{CO}_2\text{-H}_2\text{O}$ solutions between 0 and 90°C, and an evaluation of the aqueous model for the system $\text{CaCO}_3\text{-CO}_2\text{-H}_2\text{O}$. *Geochim. Cosmochim. Acta* 46, 1011–1040. <https://doi.org/0016-7037/82/061011-3OSO3.00/0>
- Purgstaller, B., Dietzel, M., Baldermann, A., Mavromatis, V., 2017. Control of temperature and aqueous $\text{Mg}^{2+}/\text{Ca}^{2+}$ ratio on the (trans-)formation of ikaite. *Geochim. Cosmochim. Acta* 217, 128–143. <https://doi.org/10.1016/j.gca.2017.08.016>
- Rietveld, H.M., 1969. A profile refinement method for nuclear and magnetic structures. *J. Appl. Crystallogr.* 2, 65–71. <https://doi.org/10.1107/S0021889869006558>
- Sekkal, W., Zaoui, A., 2013. Nanoscale analysis of the morphology and surface stability of calcium carbonate polymorphs. *Sci. Rep.* 3, 1587. <https://doi.org/10.1038/srep01587>
- Shahar, A., Bassett, W.A., Mao, H., Chou, I.-M., Mao, W., 2005. The stability and Raman spectra of ikaite, $\text{CaCO}_3 \cdot 6\text{H}_2\text{O}$, at high pressure and temperature. *Am. Mineral.* 90, 1835–1839. <https://doi.org/10.2138/am.2005.1783>
- Stockmann, G., Tollefsen, E., Skelton, A., Brüchert, V., Balic-Zunic, T., Langhof, J., Skogby, H., Karlsson, A., 2018. Control of a calcite inhibitor (phosphate) and temperature on ikaite precipitation in Ikka Fjord, southwest Greenland. *Appl. Geochem.* 89, 11–22. <https://doi.org/10.1016/j.apgeochem.2017.11.005>
- Swainson, I.P., Hammond, R.P., 2001. Ikaite, $\text{CaCO}_3 \cdot 6\text{H}_2\text{O}$: Cold comfort for glendonites as paleothermometers. *Am. Mineral.* 86, 1530–1533. <https://doi.org/10.2138/am-2001-11-1223>
- Tollefsen, E., n.d. Rapport pilotprojektet ikait som övergångsmineral i kollagrings processer.
- Tollefsen, E., Balic-Zunic, T., Mörth, C.-M., Brüchert, V., Lee, C.C., Skelton, A., 2020. Ikaite nucleation at 35 °C challenges the use of glendonite as a paleotemperature indicator. *Sci. Rep.* 10, 8141. <https://doi.org/10.1038/s41598-020-64751-5>
- Tollefsen, E., Skelton, A., 2020. Method for preparation of Ikaite Crystals and for Carbon Capture and Storage. SE 543 928 C2.
- Tollefsen, E., Stockmann, G., Skelton, A., Mörth, C.-M., Dupraz, C., Sturkell, E., 2018. Chemical controls on ikaite formation. *Mineral. Mag.* 82, 1119–1129. <https://doi.org/10.1180/mgm.2018.110>
- Trampe, E.C.L., Larsen, J.E.N., Glaring, M.A., Stougaard, P., Kühl, M., 2016. In situ dynamics of O_2 , pH, light, and photosynthesis in ikaite tufa columns (Ikka Fjord, Greenland)—A unique microbial habitat. *Front. Microbiol.* 7. <https://doi.org/10.3389/fmicb.2016.00722>
- Vickers, M., Watkinson, M., Price, G.D., Jerrett, R., 2018. An improved model for the ikaite-glendonite transformation: evidence from the Lower Cretaceous of Spitsbergen, Svalbard. *Nor. J. Geol.* <https://doi.org/10.17850/njg98-1-01>

- Vickers, M.L., Lengger, S.K., Bernasconi, S.M., Thibault, N., Schultz, B.P., Fernandez, A., Ullmann, C.V., McCormack, P., Bjerrum, C.J., Rasmussen, J.A., Hougård, I.W., Korte, C., 2020. Cold spells in the Nordic Seas during the early Eocene Greenhouse. *Nat. Commun.* 11, 4713. <https://doi.org/10.1038/s41467-020-18558-7>
- Vickers, M.L., Price, G.D., Jerrett, R.M., Sutton, P., Watkinson, M.P., FitzPatrick, M., 2019. The duration and magnitude of Cretaceous cool events: Evidence from the northern high latitudes. *GSA Bull.* 131, 1979–1994. <https://doi.org/10.1130/B35074.1>
- Vickers, M.L., Vickers, M., Rickaby, R.E.M., Wu, H., Bernasconi, S.M., Ullmann, C.V., Bohrmann, G., Spielhagen, R.F., Kassens, H., Pagh Schultz, B., Alwmark, C., Thibault, N., Korte, C., 2022. The ikaite to calcite transformation: Implications for palaeoclimate studies. *Geochim. Cosmochim. Acta* 334, 201–216. <https://doi.org/10.1016/j.gca.2022.08.001>
- Zhang, Y., Dawe, R.A., 2000. Influence of Mg²⁺ on the kinetics of calcite precipitation and calcite crystal morphology. *Chem. Geol.* 163, 129–138. [https://doi.org/10.1016/S0009-2541\(99\)00097-2](https://doi.org/10.1016/S0009-2541(99)00097-2)

Appendices

Appendix A: Experimental results

Sample name	Seawater	Mixed water	Temp of exp	Volume of precipitat	Seawater pH	Seawater Temp °C	Mixed water pH	Mixed water Temp °C	Reactant fluid pH	Reactant fluid Temp °C	Filtered Residue pH	Filtered Residue Temp °C	Precipitate gram
Exp 3-22-a	Styrsö	2:1 Batch 1	5	653.5	8.84	7.90	10.41	8.00	10.20	11.30	10.09	10.20	0.06
Exp 3-22-b	Styrsö	3-22-a residue	5	639.3	8.86	8.30	10.09	10.20	9.89	11.30	9.85	7.00	0.33
Exp 3-22-c	Styrsö	3-22-b residue	5	626.1	8.83	7.20	9.85	7.00	9.68	10.40	9.49	7.00	0.06
Exp 3-22-d	Styrsö	3-22-c residue	5	580.3	8.70	7.10	9.49	7.00	9.31	9.90	9.20	8.90	-
Exp 4-22-a	Styrsö	2:1 Batch 2	20	696.5	8.76	20.20	10.35	20.10	10.09	20.60	10.05	20.00	0.06
Exp 4-22-b	Styrsö	4-22-a residue	20	681.5	8.72	20.00	10.05	20.00	9.83	20.60	9.77	20.00	0.31
Exp 4-22-c	Styrsö	4-22-b residue	20	680.2	8.71	20.10	9.77	20.00	9.59	20.40	9.38	20.00	0.07
Exp 4-22-d	Styrsö	4-22-c residue	20	665.4	8.63	20.00	9.38	20.00	9.21	20.60	8.75	20.60	0.04
Exp 4-22-e	Styrsö Batch 2	4-22-d residue	20	648.4	8.63	20.50	8.75	20.60	8.68	22.00	8.66	7.00	-
Exp 5-22-a	Styrsö Batch 2	2:1 Batch 3	20	655.7	8.60	20.00	10.34	20.00	10.05	20.50	9.99	20.00	0.06
Exp 6-22-a	Styrsö Batch 2	2:1 Batch 4	5	597.1	8.86	7.80	10.44	6.90	10.15	10.40	10.11	7.10	0.05
Exp 5-22-b	Styrsö Batch 2	5-22-a residue	20	653.2	8.66	19.90	9.99	20.00	9.79	20.50	9.74	19.90	0.28
Exp 6-22-b	Styrsö Batch 2	6-22-a residue	5	588.8	8.61	7.00	10.11	7.10	9.92	9.80	9.85	6.70	0.22
Exp 5-22-c	Styrsö Batch 2	5-22-b residue	20	648.6	8.65	19.90	9.74	19.90	9.57	20.40	9.29	20.00	0.07
Exp 6-22-c	Styrsö Batch 2	6-22-b residue	5	592.8	8.67	6.80	9.85	6.70	9.65	9.80	9.52	6.90	0.16
Exp 5-22-d	Styrsö Batch 2	5-22-c residue	20	684	8.58	20.00	9.29	20.00	9.15	20.60	8.77	20.10	0.04
Exp 6-22-d	Styrsö Batch 2	6-22-c residue	5	608.2	8.70	6.80	9.52	6.90	9.28	9.80	9.18	8.00	0.00
Exp 5-22-e	Styrsö Batch 2	6-22-d residue	20	680.1	8.55	20.00	8.77	20.10	8.69	20.30	8.74	8.00	-

Appendix B: Results from PhreeqC analysis

Mineral	ACC	Aragonite	Calcite	Calcite_(P&B)	Hydromagnesite	Ikaite	Ikaite_(C)	Lansfordite	Monohydrocalcite	Nesquehonite	Vaterite
Sample											
3-22-a	10.28	2.37	2.52	2.51	5.4	1.17	1.13	0.7	1.72	-0.48	1.89
3-22-b	10.18	2.27	2.42	2.41	5.28	1.07	1.03	0.72	1.63	-0.46	1.79
3-22-c	9.95	2.05	2.19	2.19	4.13	0.84	0.8	0.5	1.4	-0.67	1.56
3-22-d	9.77	1.86	2.01	2	2.77	0.65	0.61	0.3	1.21	-0.88	1.38
3-22-e	9.61	1.71	1.85	1.85	1.45	0.5	0.46	0.07	1.06	-1.1	1.23
4-22-a	11.18	2.35	2.49	2.45	7.05	0.68	0.7	0.48	1.65	-0.11	1.87
4-22-b	11.12	2.29	2.43	2.39	7.17	0.62	0.64	0.53	1.59	-0.05	1.81
4-22-c	10.95	2.13	2.27	2.23	6.28	0.45	0.47	0.38	1.43	-0.2	1.65
4-22-d	10.79	1.96	2.11	2.07	4.93	0.29	0.31	0.19	1.27	-0.39	1.49
4-22-e	10.44	1.61	1.75	1.71	2.09	-0.07	-0.05	-0.25	0.91	-0.84	1.13
4-22-f	9.3	1.39	1.54	1.53	-1.1	0.18	0.14	-0.32	0.74	-1.49	0.91
5-22-a	11.16	2.33	2.48	2.43	6.94	0.66	0.68	0.46	1.64	-0.13	1.85
5-22-b	11.08	2.25	2.4	2.36	6.92	0.58	0.6	0.49	1.56	-0.09	1.78
5-22-c	10.98	2.15	2.29	2.25	6.38	0.48	0.5	0.43	1.45	-0.16	1.67
5-22-d	10.7	1.87	2.01	1.97	4.33	0.2	0.21	0.08	1.17	-0.5	1.39
5-22-e	10.4	1.57	1.72	1.68	1.86	-0.1	-0.08	-0.31	0.88	-0.9	1.1
5-22-f	9.31	1.41	1.55	1.55	-0.9	0.2	0.16	-0.31	0.76	-1.48	0.92
6-22-a	10.26	2.35	2.5	2.5	5.29	1.15	1.11	0.67	1.71	-0.5	1.87
6-22-b	10.19	2.28	2.43	2.42	5.35	1.08	1.04	0.74	1.64	-0.43	1.8
6-22-c	9.97	2.07	2.21	2.21	4.28	0.86	0.82	0.54	1.42	-0.63	1.58
6-22-d	9.84	1.93	2.08	2.07	3.15	0.72	0.68	0.38	1.28	-0.79	1.45
6-22-e	9.62	1.71	1.86	1.85	1.28	0.51	0.47	0.04	1.07	-1.13	1.23

* Saturation index (SI) = IAP/K

Appendix C: Results from PhreeqC analysis

	ICP-OES	Input	Theoretical precipitation			Experimental	
	Ca Mmol/kg	Ca Mmol/kg	Ca mmol/kg	Ikaite mg/kg	Ikaite g/kg	Ikaite g/kg	Difference
3-22-a	0.224	2.750	2.526	525.833	0.526	0.097	0.429
3-22-b	0.423	2.750	2.327	484.380	0.484	0.523	-0.039
4-22-a	0.211	2.750	2.539	528.541	0.529	0.080	0.449
4-22-b	0.355	2.750	2.395	498.645	0.499	0.461	0.038
5-22-a	0.224	2.600	2.376	494.702	0.495	0.090	0.404
5-22-b	0.400	2.600	2.200	457.982	0.458	0.428	0.030
6-22-a	0.235	2.600	2.365	492.346	0.492	0.079	0.413
6-22-b	0.360	2.600	2.240	466.396	0.466	0.381	0.085

Ikaite molar mass	208.174
-------------------	---------

	Ca mmol/kg	Input into mixture
Sw1	5.500	2.750
Sw2	5.200	2.600

Average missing precipitate		
	Total	Average
Intial experiment	1.695	0.424
First recycling	0.115	0.0287

Appendix D: Calculation support for the sequestration in % of CO₂

Molar mass	
Na ₂ CO ₃	105.988
NaHCO ₃	84.006
Ikaite	208.096
MHC*	103.110
Aragonite	100.086
CO ₂	44.009

Calculation for introduced CO ₂ in g/kg					
	M	g/kg	CO ₂ g/kg	L	2:1 g/kg
Na ₂ CO ₃	0.1	10.599	4.401	0.667	2.934
NaHCO ₃	0.1	8.401	4.401	0.333	1.467
			Total CO ₂ g/kg		4.401

* Monhydrocalcite

Sample name	From 2022 Ikaite experiments tab			XRD results in %			CO ₂ sequestered g/kg				Remaining CO ₂	Sequestration %
	V in kg of liquid	Grams of precipitate	Precipitate g/kg	Ikaite	Monohydrocalcite	Aragonite	Ikaite	Monohydrocalcite	Aragonite	Sum of CO ₂ Seq		
Series 1, 5°												
3-22-a	0.654	0.063	0.097	100%			0.020	0.000	0.000	0.020	4.380	0.5%
3-22-b	0.639	0.335	0.523	89%	11%		0.098	0.025	0.000	0.123	4.257	2.8%
3-22-c	0.626	0.057	0.091	37%	63%		0.007	0.024	0.000	0.031	4.226	0.7%
3-22-d	0.580	0.000	0.000				0.000	0.000	0.000	0.000	4.226	0.0%
Series 2, 20°												
4-22-a	0.697	0.056	0.080	100%			0.017	0.000	0.000	0.017	4.384	0.4%
4-22-b	0.682	0.314	0.461	88%	12%		0.086	0.024	0.000	0.109	4.275	2.6%
4-22-c	0.680	0.074	0.109		86%	14%	0.000	0.040	0.007	0.047	4.228	1.1%
4-22-d	0.665	0.042	0.063			100%	0.000	0.000	0.028	0.028	4.200	0.7%
4-22-e	0.648	0.000	0.000				0.000	0.000	0.000	0.000	4.200	0.0%
Series 3, 5°												
6-22-a	0.597	0.047	0.079	100%			0.017	0.000	0.000	0.017	4.384	0.4%
6-22-b	0.589	0.224	0.381	100%			0.081	0.000	0.000	0.081	4.304	1.9%
6-22-c	0.593	0.155	0.262	73%	18%	9%	0.040	0.020	0.010	0.071	4.233	1.7%
6-22-d	0.608	0.000	0.001				0.000	0.000	0.000	0.000	4.233	0.0%
Series 4, 20°												
5-22-a	0.656	0.059	0.090	100%			0.019	0.000	0.000	0.019	4.382	0.4%
5-22-b	0.653	0.279	0.428	82%		18%	0.074	0.000	0.034	0.108	4.274	2.5%
5-22-c	0.649	0.066	0.102		56%	44%	0.000	0.024	0.020	0.044	4.230	1.0%
5-22-d	0.684	0.042	0.061			100%	0.000	0.000	0.027	0.027	4.203	0.6%
5-22-e	0.680	0.000	0.000				0.000	0.000	0.000	0.000	4.203	0.0%